Organic complexation of rare earth elements in natural waters: evaluating model calculations from ultrafiltration data

Olivier Pourret, Mélanie Davranche, Gérard Gruau, Aline Dia

ORGANIC COMPLEXATION OF RARE EARTH ELEMENTS IN NATURAL WATERS: EVALUATING MODEL CALCULATIONS FROM ULTRAFILTRATION DATA

Running head: Organic complexation of REE in natural waters

Olivier Pourret*, Mélanie Davranche, Gérard Gruau and Aline Dia

CAREN, Géosciences Rennes, UMR CNRS 6118, Campus de Beaulieu

35042 RENNES Cedex, France

Keywords: Rare earth elements, dissolved organic matter, speciation modelling, natural waters, ultrafiltration

**Author to whom correspondence should be addressed (olivier.pourret@univ-rennes1.fr).*

Abstract – The Stockholm Humic Model (SHM) and Humic Ion-Binding Models V and VI were compared for their ability to predict the role of dissolved organic matter (DOM) in the speciation of rare earth elements (REE) in natural waters. Unlike Models V and VI, SHM is part of a speciation code that also allows us to consider dissolution/precipitation, sorption/desorption and oxidation/reduction reactions. In this context, it is particularly interesting to test the performance of SHM. The REE specific equilibrium constants required by the speciation models were estimated using linear free-energy relationships (LFER) between the first hydrolysis constants and the stability constants for REE complexation with lactic and acetic acid. Three datasets were used for the purpose of comparison: (i) World Average River Water (Dissolved Organic Carbon (DOC) = 5 mg L^{-1}), previously investigated using Model V, was reinvestigated using SHM and Model VI; (ii) two natural organic-rich waters (DOC = 18-24 mg L^{-1}), whose REE speciation has already been determined with both Model V and ultrafiltration studies, were also reinvestigated using SHM and Model VI; finally, (iii) new ultrafiltration experiments were carried out on samples of circumneutral-pH (pH = 6.2-7.1), organic-rich (DOC = 7-20 mg L^{-1}) groundwaters from the Kervidy-Naizin and Petit-Hermitage catchments, western France. The results were then compared with speciation predictions provided by Model VI and SHM, successively. When applied to World Average River Water, both Model VI and SHM yield comparable results, confirming the earlier finding that a large fraction of the dissolved REE in rivers occurs as organic complexes This implies that the two models are equally valid for calculating REE speciation in low-DOC waters at circumneutral-pH. The two models also successfully reproduced ultrafiltration results obtained for DOC-rich acidic groundwaters and river waters. By contrast, the two models yielded different results when compared to newly obtained ultrafiltration results for DOC-rich (DOC > 7 mg L^{-1}) groundwaters at circumneutral-pH, with Model VI predictions being closer to the ultrafiltration data than SHM. Sensitivity analysis indicates that the "active DOM parameter" (i.e., the proportion of DOC that can effectively complex with REE) is a key parameter for both Model VI and SHM. However, a survey of

ultrafiltration results allows the "active DOM parameter" to be precisely determined for the newly ultrafiltered waters studied here. Thus, the observed discrepancy between SHM predictions and ultrafiltration results cannot be explained by the use of inappropriate "active DOM parameter" values in this model. Save this unexplained discrepancy, the results presented in this study demonstrate that both Model VI and SHM can provide reliable estimates of REE speciation in organic-rich waters. However, it is essential to know the proportion of DOM that can actively complex REE before running these two speciation models.

1. INTRODUCTION

The aquatic geochemistry of rare earth elements (REE) has been the subject of numerous studies over the past two decades (Elderfield and Greaves, 1982; De Baar et al., 1988; Elderfield et al., 1990; De Baar et al., 1991; Smedley, 1991; Gosselin et al., 1992; Sholkovitz, 1995; Byrne and Sholkovitz, 1996; Johannesson et al., 1997; 2000; Johannesson and Hendry, 2000; Janssen and Verweij, 2003; Nelson et al., 2004). However, it is difficult to assess the extent to which REE patterns in natural waters are controlled by the source rocks (Johannesson et al., 1999; Dia et al., 2000; Aubert et al., 2001). Processes such as REE complexation by inorganic ligands, or REE adsorption onto solid mineral phases, can fractionate the REE (e.g., Johannesson et al., 1999; Coppin et al., 2002). There is also some evidence that REE adsorption onto Fe- and Mn-oxides may lead to negative Ce anomalies in waters due to the oxidative scavenging of Ce onto these metallic oxides (Viers et al., 1997; Dupré et al., 1999; Dia et al., 2000; Davranche et al., 2004; Gruau et al., 2004; Davranche et al., 2005). Above all, REE complexation with natural organic ligands may be of prime importance in controlling REE fractionation in natural waters, as inferred from recent ultrafiltration and electrochemical studies of organic-rich waters (Tanizaki et al., 1992; Viers et al., 1997; Dupré et al., 1999; Dia et al., 2000; Ingri et al., 2000; Johannesson et al., 2004).

Consequently, it is essential to develop models to predict the complexation of REE with dissolved organic matter (DOM). For that purpose, we require REE binding constants for REE-proton exchange with humic matter (HM). These constants can be experimentally determined, either for individual REE (e.g., Bidoglio et al., 1991; Moulin et al., 1992; Lead et al., 1998; Lippold et al., 2005) or for the whole REE series (Yamamoto et al., 2005; Sonke and Salters, 2006; Yamamoto et al., 2006). However, experimentally determined REE constants may be difficult to use because of differences in the pH and/or ionic strength conditions of the experiments (Bidoglio et al., 1991; Moulin et al., 1992; Lead et al., 1998; Lippold et al., 2005) or

due to differences in the REE/HM ratio of the experimental solutions (Yamamoto et al., 2005; Sonke and Salters, 2006). An indirect method is to estimate the required Lanthanide-humic (LnHM) constants using the Linear Free Energy Relationships (LFER) existing between metal-HM complexation and the stability constants for metal-lactic and metal-acetic acid complexation. These LnHM values can then be put into thermodynamic models aimed at predicting metal complexation with HM. The ability of the models to predict REE complexation with DOM can then be established by comparing model results with ultrafiltration data. The most successful attempt along these lines was made by Tang and Johannesson (2003), who applied the indirect method to test the ability of the well-known metal-HM speciation code Humic Ion-Binding Model V (Tipping, 1994) to predict REE complexation with DOM. Comparisons between model predictions and ultrafiltration results for six natural water samples were then used by these authors (op. cit.) to validate both the estimated LnHM and the model. Applying Model V to World Average River Water, Tang and Johannesson (2003) predicted that LnHM complexes are the principal carriers of REE in the dissolved (i.e., <0.2 μm) fraction of river waters.

However, Model V is exclusively a speciation model that does not take account of other reactions (i.e., dissolution/precipitation, adsorption/desorption, oxidation/reduction) that are also important in controlling the REE distribution in waters. In this study, we test the ability of the Stockholm Humic Model (SHM) to predict REE complexation by HM (Gustafsson, 2001a; Gustafsson et al., 2003). This model was selected because it is part of a full chemical equilibrium model that allows modelling of all the above reactions (Visual MINTEQ; Gustafsson, 2001b). The aim of our study is also to compare SHM with Model VI, which is the latest version of the Humic Ion Binding Model (Tipping, 1998). REE constants were estimated using the above described indirect LFER method. For purposes of comparison, we used the following three-step approach: firstly, World Average River Water, previously investigated using Model V by Tang and Johannesson (2003), was reinvestigated successively using Model VI and SHM. Secondly, we used both SHM and Model VI to reinvestigate two of the six ultrafiltered organic-rich natural

waters used by Tang and Johannesson (2003) to validate Model V. Finally, new ultrafiltration experiments were conducted using organic-rich (Dissolved Organic Carbon (DOC) 7-20 mg L^{-1}) groundwaters with circumneutral-pH (pH = 6.2-7.1) from the Kervidy-Naizin and Petit-Hermitage catchments, western France, and the results were compared with predictions from Model VI and SHM . Hence, the present study is also a new step in assessing the ability of the Humic Ion Binding Model to predict REE complexation by organic matter in natural waters. So far, this model has been compared to only a limited number of ultrafiltration results (Tang and Johannesson, 2003).

2. MATERIALS AND METHODS

In this paper, we use the term *organic matter-bound REE solution complex* in the same way as in Tang and Johannesson (2003), namely, to include REE complexed to both low- and high-molecular weight (MW) organic matter.

2.1. Description of models

Humic Ion-Binding Model VI (here referred to as Model VI) is the latest version of a model developed by Tipping and co-workers in the early 1990s (Tipping and Hurley, 1992; Tipping, 1994; Tipping, 1998). Model VI is a discrete site-electrostatic model for proton and metal ion interactions with fulvic (FA) and humic (HA) acids. The thermodynamic basis of the model has been presented and discussed in detail elsewhere (e.g., Tipping, 1998). Briefly, the model assumes that proton and metal complexation by organic matter involve two types of discrete sites (Type A and Type B) that have separate intrinsic binding constants for metals: log K_{MA} and log K_{MB}. By considering results from many datasets, we obtain a universal average value of ΔLK_1, and can establish a correlation between log K_{MB} and log K_{MA} (Tipping, 1998). Thus, we only require one single adjustable parameter (log K_{MA}) to fully describe metal binding in Model VI.

The parameters necessary to run the model are presented in Table EA1-Electronic Annex (based on Tipping, 1998). As shown by Tipping (1998) and Tipping et al. (2002), updating Model V to Model VI leads in many cases to an overall improvement of the predictive power of the model.

The Stockholm Humic Model (SHM) is an integral part of the chemical equilibrium model Visual MINTEQ (Gustafsson, 2001b), which enables modelling of solution speciation along with adsorption/desorption, dissolution/precipitation and redox reactions. The principles of SHM have been fully presented and discussed elsewhere by Gustafsson (2001a) and Gustafsson et al. (2003). Where applicable, Gustafsson (2001a) gave the same symbols to denote SHM parameters as those used for corresponding parameters in Models VI, for sake of consistency. SHM is a discrete-ligand model in which the FA and HA are assumed to have eight proton-binding sites with distinct acid-base characteristics. In this model, seven adjustable parameters (n_A, n_B, log K_A, log K_B, ΔpK_A, ΔpK_B and g_f) are required to describe the proton dissociation reaction. Table EA2-Electronic Annex lists the fixed values that Gustafsson (2001a) derived for these seven parameters for FA and HA. In the present study, we select the generic values for these parameters listed in the "shmgeneric.mdb" database, since they are average values obtained from a large number of aquatic FA and HA samples (Gustafsson, 2001b). Three parameters are normally required with SHM to model the complexation of metals with organic matter, i.e., the monodentate complexation constant K_{Mm}, the bidentate complexation constant K_{Mb}, and the ΔLK_2 parameter, which determines the degree of binding site heterogeneity. Gustafsson (2001a) demonstrated that trivalent cation (e.g., Al) organic complexation is better fitted if only bidentate binding is involved. Therefore, in practice, only a single adjustable parameter (log K_{Mb}) is necessary to fully describe trivalent metal complexation by HM in natural waters (Gustafsson, 2001b).

However, results from both SHM and Model VI depend on the values of the ΔLK_2 parameter (i.e., the distribution term that modifies the strengths of complexation sites) which is input in models. Because SHM and Model VI are different in a number of respects, a ΔLK_2 value adopted

from Model VI cannot be expected to yield similar good fits for SHM. In the following we use the ΔLK_2 values which were optimized by fitting published datasets (Milne et al., 2003) for SHM (namely 1.3; Gustafsson, 2001b) or from a correlation with the equilibrium constant for complexation of the metal with NH_3 for Model VI (0.29; Lead et al., 1998; Tipping, 1998). The ΔLK_2 values are constrained to be identical for the whole REE series as REE are known for their chemical similarity.

2.2. Estimating constant values for the REE

As pointed out in the introduction, we used the LFER method to estimate the specific binding constants necessary to run Model VI and SHM. The LFER method is based on Tipping's observation (Tipping, 1994; Tipping, 1998) that a LFER exists between log K_{MA} and log K for metal-lactic acid (LA) and metal-acetic acid (AA) complexation. Moreover, since this author (*op. cit.*) also notes a relation between log K_{MA} and the first hydrolysis (OH) constants for metal (denoted here as log K(AA), log K(LA) and log K(OH)), the LFER can be used to estimate log K_{MA}(REE) from published values of log K(REE-AA), log K(REE-LA) and log K(REE-OH). The same approach can be used to estimate log K_{Mb}(REE), the only difference being the assumption that the metal complexing capacity of one ligand with two functional groups (as expressed by K_{Mb}) is similar to the metal complexing capacity of two ligands carrying only one functional group each (as expressed by K_2).

Tables 1 and 2 list log K_{MA} and log K_{Mb} values describing the complexation of numerous metals with HA and FA (data from Tipping, 1998, and Gustafsson, 2001b), along with published log K(AA), log K(LA), log K(OH), log K_2(AA), log K_2(LA) and log K_2(OH) for the same metals (values from NIST Database; Martell and Smith, 1998). Studentized residuals (i.e., the residual divided by its standard deviation; Ramsey, 1969) were used to detect and remove outlier cations (i.e., Cd and Th). The values of log K_{MA} and log K_{Mb} show good linear correlations with their

hydrolysis constants, as well as the constants for LA and AA complexation (Figs. 1 and 2). The linear regression curves and correlation coefficients describing these relationships are as follows:

$$\log K_{MA}\,(HA) = 0.76 \log K\,(LA) - 0.21 \qquad R^2 = 0.80 \qquad (1)$$

$$\log K_{MA}\,(FA) = 0.52 \log K\,(LA) + 0.58 \qquad R^2 = 0.78 \qquad (2)$$

$$\log K_{MA}\,(HA) = 1.03 \log K\,(AA) - 0.43 \qquad R^2 = 0.80 \qquad (3)$$

$$\log K_{MA}\,(FA) = 0.75 \log K\,(AA) + 0.36 \qquad R^2 = 0.87 \qquad (4)$$

$$\log K_{MA}\,(HA) = 0.24 \log K\,(OH) + 0.32 \qquad R^2 = 0.78 \qquad (5)$$

$$\log K_{MA}\,(FA) = 0.17 \log K\,(OH) + 0.91 \qquad R^2 = 0.83 \qquad (6)$$

$$\log K_{Mb} = 1.89\ \log K_2\,(LA) - 15.13 \qquad R^2 = 0.81 \qquad (7)$$

$$\log K_{Mb} = 1.49 \log K_2\,(AA) - 11.80 \qquad R^2 = 0.82 \qquad (8)$$

$$\log K_{Mb} = 0.57 \log K_2\,(OH) - 13.86 \qquad R^2 = 0.73 \qquad (9)$$

These equations were subsequently employed to estimate log K_{MA} (Table 3) and log K_{Mb} (Table 4), using the log K(AA), log K(LA), log K(OH), log K_2(AA), log K_2(LA) and log K_2(OH) values listed for REE in the NIST Database (Martell and Smith, 1998; except log K(OH) listed in Klungness and Byrne, 2000; Figs. 1 and 2). However, as shown by Tables 3 and 4, the estimated values of log K_{MA} and log K_{Mb} vary depending on the equation used. To establish which sets of estimated values are more appropriate, we used the method of Tang and Johannesson (2003) to compare them with log K_{MA} and log K_{Mb}, which were determined by fitting Model VI and SHM to the available experimental data (Tipping 1998; Gustafsson, 2001b). For purposes of comparison, we only considered "best-fit" values of log K_{MA} and log K_{Mb} (rms errors < 0.1), which limits the comparison solely to Eu and Dy (Tipping, 1998; Lead et al., 1998; Gustafsson, 2001b). It is clear that the log K_{MA} values are too low when estimated from the LFER based on first hydrolysis constants (e.g., log K_{MA}=1.79 for Eu-HA complexation using Eqn. 5, as against 2.10 using model fits). The same is true for Dy complexation by HA and FA (e.g., log K_{MA}=1.83

for Dy-HA complexation as obtained from Eqn. 5, as against 2.9 using model fits). However, this does apply to the log K_{MA} values estimated from Eqns. 1 to 4, where estimated values for Eu and Dy are close to the fitted experimental data (e.g., 2.47 and 2.44 for Eu-FA complexation using Eqn. 2 and 4, respectively, as against 2.36 from model fits). The log K_{MA} estimates derived from the first hydrolysis constant LFER appear much too low. Whatever the reason, the observed discrepancy between estimates derived from Eqn. 5 and 6 and fits of experimental data leads us to eliminate these two equations from our procedure for estimating constants.

However, log K_{MA} values estimated from Eqn. 1 to 4 are quite different for the HREE (on average, standard deviation are as high as 0.41). Recently published experimental results for REE complexation with FA and HA (Yamamoto et al., 2005; 2006) suggest that the log K values for REE complexation with HM should vary across the REE series in an analogous way to the log K values for AA. Moreover, Wood (1993) pointed out that AA likely represents a model system for simple carboxylic sites on more complex organic matter, such as HM. Carboxylic groups could thus be the major sites by which REE are bound to HM (Yamamoto et al., 2005; 2006).

Log K_{Mb} values estimated using Eqns. 7, 8 and 9 strongly differ from one another: by approximately two orders of magnitude for the LREE and by four orders of magnitude for the HREE (Table 4). As with the log K_{MA} values, log K_{Mb} can be estimated by comparing the values obtained for Eu with the log K_{Mb} values determined by fitting SHM to Eu experimental results (Gustafsson, 2001b). By using the second hydrolysis constants, we obtain a log K_{Mb} value of -7.36 for Eu that is dramatically low compared to -4.7 from the model fit (see Gustafsson, 2001b). By contrast, the log K_{Mb} values estimated for Eu using Eqns. 7 and 8 (-4.15 and -4.79 from Eqn. 7 and 8, respectively) are closer to the fitted experimental data for this REE than the value of -4.65 derived from the model fit (Gustafsson, 2001b). However, as with the log K_{MA} values, we note that the log K_{Mb} values estimated using Eqns. 7 and 8 agree better with one another for the LREE and MREE than for the HREE (the standard deviation varies up to 1.89 for the latter).

Bearing in mind that metal complexation with AA is probably a better analogy for REE complexation with HM than metal complexation with LA (see discussion above), in the following, we adopt the log K_{Mb} values estimated from Eqn. 8. To conclude, we should point out that, due to the smaller amount of experimental data, the AA LFER used to estimate log K_{Mb} values is less well constrained than the AA LFER used to estimate log K_{MA}. Thus, we can expect that modelling results derived from SHM are likely to be accompanied by larger uncertainties than Model VI predictions.

3. COMPARING THE PREDICTIVE ABILITY OF SHM AND MODELS V AND VI

Speciation calculations were performed using the computer programs WHAM 6 (Version 6.0.13) for Model VI, and Visual MINTEQ (Version 2.40) for SHM. Each model was modified by building a database that included our adopted log K_{MA} and log K_{Mb} values for REE complexation with HM, along with well-accepted infinite-dilution (25°C) stability constants for REE inorganic complexes (hydroxide, sulphate and carbonate; Klungness and Byrne, 2000; Luo and Byrne, 2004; Schijf and Byrne, 2004). Up-to-date, default values of log K_{MA}, log K_{Mm} and log K_{Mb} were used for competing cations (Tipping, 1998; Gustafsson, 2001b). As oxyhydroxide precipitation reactions can not be modelled by Model VI, they were not considered in SHM modelling. In our simulations, we do not take into account the binding of the first hydrolysis product to HM. This choice is supported by the fact that (i) all the tested waters have pH < 7; yet, it is well established that the proportion of Ln-OH complexes and thus Ln-OH-HM complexes may become important only for water having pH > 8 (Maes et al., 1988); (ii) even for alkaline waters, recent model calculations show that REE speciation can be reasonably well captured by only considering Ln^{3+} complexation with HM (Pourret et al., 2007).

In the speciation calculations presented here for World Average River Water, and Mengong and Mar2 samples, we follow the same assumptions as Tang and Johannesson (2003), i.e., (i) the

DOM/DOC ratio of all samples is taken to be equal to 2; (ii) 50% of the DOM is considered to consist of HM able to complex the REE, the remaining 50% comprising simple organic acids that cannot form REE complexes. Thus, the active-DOM/DOC ratio (referred to here as the "active DOM parameter") is taken as equal to unity for these samples.

3.1. World Average River Water

We applied the same DOC (5 mg L^{-1}), major ion, Fe and Al concentrations as those used by Tang and Johannesson (2003) in their earlier modelling of REE speciation in World Average River Water (see Table 11 in Tang and Johannesson, 2003). We also followed their assumption that 80% of the HM in this sample is present as FA and 20% as HA. Thus, the DOM content of World Average River Water is 10 mg L^{-1}, of which only 5 mg L^{-1} consist of HM able to complex with the REE, with 4 mg L^{-1} (80%) present as FA, and 1 mg L^{-1} (20%) as HA. Finally, because pH has a crucial influence on REE speciation, we also investigated the REE speciation of World Average River Water as a function of varying pH, while keeping the major solute composition constant (except carbonate alkalinity varying as a function of pH). Except for the slight modification of complexation constants, our model running procedure is thus entirely comparable to that used by Tang and Johannesson (2003).

The new modelling results are shown for La, Eu, and Lu in Figs. 3 (Model VI) and 4 (SHM), respectively. Model VI calculations predict that REE occur as free species (Ln^{3+}) and sulphate complexes ($LnSO_4^+$) at acidic pH, and mainly as carbonate complexes ($LnCO_3^+$ and $Ln(CO_3)^{2-}$) at alkaline pH (Fig. 3). Based on these results, we also predict that, at circumneutral-pH conditions, the REE predominantly (i.e., >50%) occur in solution complexed with HM. More precisely, Model VI predicts that >50% of the LREE (e.g., La) occur in solution as organic complexes in the pH range between 5.2 and 9.5. For the MREE (e.g., Eu), the prediction is that >50% of the MREE occur as HM complexes in the pH range between 4.3 and 9.5. Finally, Model

VI predicts that >50% of the HREE (e.g., Lu) occur as HM complexes in the pH range between 5.4 and 7. Another important result of the model is that the pH value at which the proportion of LnHM complexes reaches a maximum decreases across the REE series, from La (pH = 7) to Lu (pH = 6). Also, model results indicate that the proportion of REE forming HM complexes is higher for the LREE and MREE (up to 95% at pH 7) than for the HREE (maximum of 60% at pH 6). All these features are consistent with Model V predictions reported previously by Tang and Johannesson (2003). The only noticeable difference is that Model VI calculates significantly higher proportions of REE complexed with organic matter under high pH conditions: for example, Model VI predicts LaHM ~60% at pH 9, whereas Model V predicts only 10% of LaHM complexes at this pH value.

As with Models V and VI, SHM predicts that the LREE and MREE occur predominantly (i.e., >50%) in solution as HM complexes at circumneutral pH conditions. By contrast, the prediction is lower for the HREE: maximum organic complexation ~40%, against ~50% with Model VI. As with Models V and VI, the pH value at which maximum REE complexation is predicted to occur also regularly decreases across the REE series, from 7.8 for La to 6.6 for Lu. However, we note three important differences with the Models V and VI results: (i) the pH at which there is a maximum proportion or REE organic complexes is about 0.75 pH unit higher with SHM (Fig. 4) than with Model VI (Fig. 3); (ii) the range of pH values over which LnHM complexes are the predominant REE species is wider with Model VI than with SHM (e.g., LaHM >50% for a range of 4.3 pH units with Model VI, as against only 3 pH units with SHM; see Figs. 3 and 4); finally, (iii) the proportion of LnHM species calculated at alkaline pH is higher with Models VI (e.g. for La, ~50% at pH 9.5; see Fig. 3) than with SHM (e.g. for La, ~40% at pH 9.5; see Fig. 4).

To sum up, predictions from Model VI and SHM confirm the two main conclusions proposed earlier by Tang and Johannesson (2003) from speciation modelling of World Average River Water, namely that (i) organic colloids are the principal REE carriers in the dissolved fraction

(i.e., <0.2 μm); and (ii) dissolved organic ligand complexes of the REE are at least as important as carbonate complexes. The results of Model VI and SHM are clearly consistent for circumneutral-pH river waters, at least in broad outline. However, on the basis of the modelled data alone, it is difficult to determine whether Models V and VI or SHM gives the most accurate description of REE speciation in river waters. Only experimental studies involving direct measurement of the REE speciation in circumneutral-pH rivers will be able to decide which model is in better agreement with reality; for example, whether the proportion of LuHM complexes in these rivers is ≥50% as predicted by Models V and VI, or only ~40% as predicted by SHM.

3.2. Mengong and Mar2 samples

Mengong and Mar2 are two samples of organic-rich (DOC = 23.8 and 18.1 mg L^{-1}) acidic waters whose REE speciation was first investigated by ultrafiltration (Viers et al., 1997), and then modelled using Model V (Tang and Johannesson, 2003). Because the DOC of these waters is chiefly made up of the largest MW size fractions (Viers et al., 1997), Tang and Johannesson (2003) assumed that 85% of the DOC in these samples is composed of high MW HA, the remaining 15% containing low MW FA. The same assumption is used here. The values adopted for pH (Mengong = 4.6 and Mar2 = 5.5), as well as the major solute, DOC, Fe and Al concentrations, are those reported by Viers et al. (1997), being identical to the values used by Tang and Johannesson (2003). Table 5 lists the predicted proportions of LnHM complexes in these two water samples based on Model VI and SHM, as well as a comparison with the previous results obtained using Model V (Tang and Johannesson, 2003). Model VI predicts that between 46-90% (Mengong) and >98% (Mar2) of the REE occurring in the dissolved fraction (i.e., <0.2 μm) of these samples occurs as organic complexes, the remainder of each REE occurring as free species (Ln^{3+}). Table 5 shows a good agreement between the Model VI and Model V predictions,

the only noticeable difference being the slightly lower proportion of HREE organic complexes obtained with Model VI for the more acidic Mengong sample (Table 5; see also Table 8 in Tang and Johannesson, 2003). This difference is likely explained by our choice to use the log K_{MA} values derived from the AA LFER rather than the log K_{MA} values, which are averages of the estimates obtained using both the AA and LA LFER as described in Tang and Johannesson (2003). As shown above in the case of the World Average River Water sample, this choice shifts the LnHM stability field slightly towards higher pH values (compare our Fig. 3 and Fig. 4 in Tang and Johannesson, 2003), thereby decreasing the proportion of REE complexed with organic matter in acidic waters as predicted by the Humic Ion Binding Model.

SHM results are consistent with the predictions of Model V and VI for Mar2, while also indicating a predominance of LnHM complexes in this sample. The predicted complexation proportions based on SHM are equivalent to those predicted by Models V and VI (i.e., between 90 and 99% for SHM, compared with 98 and 100% for Model VI and 87 and 96% for Model V depending on the REE; see Table 5). By contrast, the results for Mengong are different. Indeed, SHM predicts that HM complexes should account for only 34 to 71% of each REE in solution, whereas Models VI and V predict higher complexation proportions, namely: between 46 and 90% (Table 5). For both the Mar2 and Mengong samples, the three tested models all indicate that the remainder of each REE occurs as free species (Ln^{3+}). By comparing the model predictions to the ultrafiltration results (Table 5), we can see that Model VI and SHM yield comparable agreement with ultrafiltration data for Mar2 sample (less than 10% difference). However, for the more acidic Mengong water sample, the difference between model predictions and ultrafiltration results is higher when using SHM compared with Models V and VI, i.e., between 27 and 62%, as against between 10 and 52% (Table 5).

In summary, we confirm the suggestion made earlier by Tang and Johannesson (2003) that the Humic Ion-Binding Model is reasonably good representation of REE speciation in acidic DOC-rich waters. The differences between our predictions and those reported in Tang and

Johannesson (2003) further demonstrate the sensitivity of models to the values of the stability constants that are introduced. As regards SHM, the results presented above might suggest that this model is less accurate in predicting the speciation of the REE in low-pH, organic-rich natural waters. In the present study, however, we show that the ability of SHM to predict REE speciation in this type of water depends strongly on the value of the "active DOM parameter" that is introduced into the model. By changing this value to more appropriate values than those used by Tang and Johannesson (2003), we can drastically improve the agreement between SHM and Model VI predictions, and ultrafiltration data (see Discussion section).

3.3. Kervidy-Naizin and Petit Hermitage groundwater samples

3.3.1. Ultrafiltration data

To further test the ability of SHM and Model VI to predict REE complexation with organic matter, we performed new ultrafiltration experiments on four circumneutral (pH = 6.2-7.1), organic-rich (DOC = 7-20 mg L^{-1}) groundwater samples (PF1, PF3, F7 and F14). The samples were collected from two wetlands located in the Kervidy-Naizin and Petit-Hermitage catchments, in western France. These groundwaters have already been intensively studied for their DOC and REE chemistry (Dia et al., 2000; Olivié-Lauquet et al., 2001; Gruau et al., 2004). Appendix 1 gives details on the ultrafiltration procedure and chemical analysis of these samples.

Table EA3-Electronic Annex presents the concentrations of major anions and cations, as well as major and trace cations (including REE) and DOC in the 0.2 µm filtrates, along with alkalinity and pH data. Concentrations of REE, Fe, Mn and DOC in the three ultrafiltered fractions (i.e., <30 kDa (Da = Dalton), <10 kDa and <5 kDa) are presented in Table EA4-Electronic Annex (mean of two analyses). In Fig. 5, these results are plotted on REE (Fe) vs. DOC variation diagrams.

Interpreting ultrafiltration data is not a trivial task and care must be taken to validate the speciation models before using this type of information. An inherent feature of ultrafiltration studies is the presence of mineral colloids (e.g., Fe and Mn oxyhydroxides) in the waters along with organic colloids. Some of these mineral colloids can be potentially strong competitors with organic matter for REE complexation (e.g., Fe oxyhydroxides; Bau, 1999; Dupré et al., 1999), and their presence may lead to an overestimation of the proportion of REE that are effectively complexed by HM. Thus, it is crucial to assess carefully whether the REE decrease associated with ultrafiltration of PF1, PF3, F7 and F14 waters (see Fig. 5) is accompanied solely by a decrease of the DOC content, or whether it is also correlated with a decrease in Fe concentration. It is clear that three of the four investigated water samples (i.e., PF1, F7 and F14) display a significant decrease in Fe content upon ultrafiltration (Fig. 5). However, the decrease in Fe content concerns only the 30 kDa ultrafiltration step. After this step, the Fe content is equally very low in all four samples, resulting in a marked change in the slope of the linear relationships otherwise shown on the REE vs. DOC variation diagrams (Fig. 5). This behaviour is particularly well illustrated by sample PF1, where ca. 80% of the REE and 96% of the Fe, but only 9% of the DOC, are removed during the first ultrafiltration step. Moreover, the magnitude of the change in the slope of the REE-DOC linear relationship appears to be correlated with the Fe/ΣREE ratio of the waters. The Fe/ΣREE ratio of PF1 before ultrafiltration is 991, whereas the Fe/ΣREE ratios of F7, F14 and PF3 are 984, 737 and 55, respectively. Such relationships strongly suggest that the "colloidal" REE budget of samples PF1, F7 and F14 is partly controlled by REE-bearing Fe colloids. The Fe-colloid/organic-colloid ratio in these samples decreases in following order: PF1 > F7 > F14 >> PF3.

The REE colloidal pool of samples PF1, F7 and F14 was corrected for the contribution of the Fe-colloid fraction. The Fe colloid-free REE budget of these waters can be estimated by linearly extrapolating the relationship defined by the <5 kDa, <10 kDa and <30 kDa results to the DOC content of the <0.2 μm fraction (point A in Fig. 5). The linear correlation defined by the DOC

and REE contents of the four ultrafiltered fractions of PF3 (i.e., the water sample clearly depleted in Fe colloid) suggests that the organic fractions should yield a linear correlation in the REE vs. DOC variation plots. This interpretation is supported by the fact that the REE vs. DOC correlations defined by the three Fe colloid-bearing waters (i.e., PF1, F7 and F14) yield a slope that decreases with decreasing Fe/REE ratio of the raw waters. This implies that the REE and DOC contents are linearly correlated in Fe-free waters. Another problem arises during ultrafiltration studies of organic-rich waters when there is a negative y-axis intercept for the REE vs. DOC correlation (Fig. 5). The likely interpretation for this is that (i) 100% of the REE present in the waters are bound to organic molecules and, more importantly (ii) the DOM is not composed solely of HM able to complex REE, but contains also a significant proportion of low MW organic molecules that do not complex these elements. In such waters, the key question is how to determine the amount of DOM that can complex the REE. In other words, we need to decide what value for the "active DOM parameter" should be introduced into the models. Considering the PF3 results, it is possible that this amount of active DOM could correspond to the y = 0 intercept on the x-axis obtained by linearly extrapolating the REE vs. DOC relationships (points B in Fig. 5). In so doing, we assume that all the REE are bound to HM, which is consistent with previously published ultrafiltration data (Tanikazi et al., 1992; Sholkovitz, 1995; Ingri et al., 2000). This assumption also agrees with recent observations by Johannesson et al. (2004) that all of the "dissolved" La in organic-rich waters from a swamp in south-eastern Virginia is "complexed" with organic ligands.

In the following, we assume that (i) 100% of the REE occurring in PF1, PF3, F7 and F14 waters are bound to HM; (ii) the REE remaining in the <5 kDa fraction are complexed with the low molecular FA; and (iii) the amount of REE complexed with the HA fraction corresponds to the REE content of point A minus the <5 kDa fraction. Table 6 reports the proportions of LnHA and LnFA complexes calculated in this way for the Kervidy-Naizin and Petit Hermitage groundwater samples. The average proportions of LnHA are lower for PF3 and F7 (65 and 76%,

respectively), but higher for PF1 and F14 (77 and 83%, respectively). Using these results, we estimated the LnFA/LnHA ratios of the four ultrafiltered samples as 0.30 for PF1, 0.54 for PF3, 0.31 for F7 and 0.21 for F14 (Table 6). The above calculations are strongly dependent on the validity of the correction/estimation procedures used to remove the contribution of Fe colloids and calculate the FA/HA ratio of the waters. The validity of this approach is tested below, by comparing the "corrected/estimated" ultrafiltration data with the modelled results. If the results of this test are positive - i.e., there is convergence between the modelling and ultrafiltration results - this confirms the ability of the models to predict LnHM speciation in the four investigated water samples, considering that the procedure for correction of the ultrafiltration data is independent of the modelling approach.

3.3.2. REE speciation modelling

The modelling of the Kervidy-Naizin and Petit Hermitage samples is treated differently from the samples of World Average River Water, Mengong and Mar2, since the amount of active DOM is not taken as equivalent to a common empirical value of 50% of the total DOM content, but equal to individual values calculated following the method described above. The active DOM fractions obtained in this way are as follows: 32% for PF1, 55% for PF3, 53% for F7 and 59% for F14. Using the ultrafiltration results, we also calculated the HA and FA contents necessary to run both models. The HA contents are assumed to be equal to two times the difference between the DOC contents of the <0.2 µm and <5 kDa fractions. For FA, we take the value as two times the difference between the DOC content of the <5 kDa fraction and that corresponding to point B in Fig. 5. Hence, we assume that 65, 76, 83 and 77% and 35, 24, 17 and 23% of HM is made up of FA and HA, respectively, in PF3, F7, F14 and PF1. Finally, we should bear in mind that the REE content introduced into the models corresponds to point A in Fig. 5 and not the total REE content of the sample.

Table 6 presents the model results, which are compared with corrected ultrafiltration data. The "modelled" complexation proportions reported in Table 6 include the REE partitioning between the high MW HA fraction (>5 kDa) and the low MW FA fraction (<5 kDa). Table 6 shows a good convergence between Model VI and ultrafiltration results. LnHM proportions calculated with Model VI are all higher than 97%, indicating that this model also predicts that nearly all of the REE are complexed by HM in these samples. By contrast, the convergence is of poorer quality with SHM: LnHM proportions range from 43 to 100% depending on the samples, while the remainder of the REE occurs as carbonate, sulphate or free ion species (data not shown). The higher the pH and the smaller the Fe/ΣREE ratio are the better the agreement between SHM prediction and ultrafiltration data is (see PF3 sample as an example). Ultrafiltration results are independent of the modelling predictions. Therefore, the strong convergence between ultrafiltration results and Model VI predictions is considered highly significant, providing evidence that this model can accurately predict REE complexation by organic matter in natural waters.

4. DISCUSSION

The log K_{MA} and log K_{Mb} values adopted here appear to be the most reliable values derived so far using the LFER method. By confronting Model VI and SHM predictions with published results (Viers et al., 1997) and new ultrafiltration data, we can define the range of conditions under which these models will accurately predict the complexation of REE by organic matter in natural waters. To a first approximation, modelling of World Average River Water (Tang and Johannesson, 2003) suggests that Humic Ion Binding Model and SHM could be equally valuable in modelling REE speciation in low-DOC river waters at circumneutral-pH. However, careful inspection of model results reveals that SHM predicts slightly lower organic complexation for the HREE than Models V and VI. Some disparities also occur for alkaline waters, with SHM

predicting an out-competition of the organic complexes over the carbonate complexes, which is not predicted by Model VI. However, these disparities do not really cast doubt on the ability of SHM and Models V and VI to provide a reliable description of REE speciation in rivers, considering that most rivers worldwide are characterized by circumneutral-pH values (Brownlow, 1996). By confronting the model results with ultrafiltration studies, we obtain a somewhat different picture, suggesting that Model VI could be more accurate than SHM in DOC-rich acidic ground- and river waters at circumneutral pH. This apparent poorer ability of SHM to accurately predict REE complexation with organic matter might be due to the different thermodynamic description of HM deprotonation by this model or competition effects between the REE and major dissolved cations such as Fe, Al or Ca. However, as shown below, the difference is more likely due to a higher sensitivity of SHM to the value of the "active DOM parameter", which is required as input into metal-HM complexation models. In fact, careful evaluation of the effects of this parameter on some of the above results shows that, in most cases, SHM could be as accurate as Models V and VI for predicting REE speciation. However, we first need to evaluate the possible effects of differences in HM proton dissociation and major cation competition.

4.1. Effect of HM proton dissociation

The main difference between SHM and Model VI is the electrostatic term. Model VI assumes that HM can be represented as rigid spheres of homogeneous size, carrying metal-humic binding sites on their surface with different binding strengths leading to of bidentate and tridentate binding configurations. In this model, electrostatic effects are corrected using equations based on the Debye-Hückel and Gouy-Chapman theories, assuming a homogeneous electrical double layer at the surface of each sphere (Tipping, 1998). In SHM, a discrete-site approach is employed involving eight sites of different acid strength. The bulk of the HM is considered to

form gels, which are primarily treated as impermeable spheres. The electrostatic interactions on their surfaces are modelled using equations based on the Basic Stern Model (see Gustafsson (2001a) for further details).

Due to these differences in the thermodynamic description of electrostatic effects, the two models assume a different extent of proton dissociation of HM reactive sites at a given pH. As shown in Fig. 6, Model VI assumes more electronegative HA and FA surfaces at a given pH than SHM, so the density of surface sites available for REE complexation is proportionally higher in Model VI than in SHM. This may partly account for the observed differences in model predictions: (i) indeed, modelling of World Average River Water results shows there is a shift of about 0.75 pH unit between the maximum of LnHM predicted by Model VI and SHM, which is consistent with the difference in electrostatic correction (Figs. 3 and 4); (ii) the proportions of REE complexed with organic matter in Mengong (pH = 4.6) sample are predicted to be slightly higher with Model VI than SHM, which is also consistent; (iii) calculations of REE speciation in three of the four organic-rich circumneutral-pH waters (i.e., PF1, F7 and F14) show differences between Model VI and SHM, with predicted values being at a maximum under acidic pH (i.e., F7 pH = 6.19), which is also as expected from the difference in electrostatic correction.

4.2. Effect of major competing cations (Fe, Al and Ca)

Fe, Al and Ca are known to complex strongly with HM (Dupré et al., 1999; Tipping et al., 2002), and can thus compete with REE in metal-HM complexing. As previously shown by Tang and Johannesson (2003), the presence of dissolved Fe and Al can decrease the amount of REE complexed with HM by ~10%. In the modelling calculations presented here, Fe, Al and Ca are present in solution, and the cation competitive effect is thus taken into account. The two models discussed here can be compared in terms of the relative importance of this effect by considering Table 7, which reports the proportions of Fe, Al, and Ca humic complexes predicted by Model

VI and SHM, as a function of pH. It can be seen that both SHM and Model VI predict roughly the same effect of Ca, which is by far the most abundant cation competing with REE in the three water samples considered here. However, the situation appears different for Fe and Al. We should note two important points: (i) the proportion of Al-HM complexes predicted to occur in circumneutral-pH waters is much higher with SHM than with Model VI; (ii) SHM predicts a much higher competition of the REE with Fe for acidic waters than Model VI. To quantify the effects of the stronger Fe and Al competition imposed by SHM on REE complexation with HM, we re-investigated the four newly ultrafiltered circumneutral-pH water samples (i.e., PF1, PF3, F7 and F14) with this model, assuming no Al and Fe in solution. The results indicate that almost all of the REE are bound to HM (~100%). On the other hand, when Fe and Al are included in the model, the LnHM species are predicted to account for 47 to 100% of each REE (depending on the sample; see Table 6). Consequently, SHM appears more sensitive to cation competition than Model VI. The reason for this difference is not clear, as the constants for Al, Fe and Ca used into the two models are derived from the same database (Tipping, 1998; Gustafsson and van Schaik, 2003).

4.3. Effect of the "active DOM parameter" value

Apart from the deprotonation and cation competition effects described above, and despite the effects on the uncertainty of log K_{MA} and log K_{Mb} values (see Tang and Johannesson, 2003 for a detailed discussion of the effect of constant uncertainty on Model V), differences in model predictions could result from the use of different values for the "active DOM parameter". In the speciation calculations presented below for World Average River Water and the Mengong and Mar2 samples, we considered as Tang and Johannesson (2003) that the amount of active DOM in these samples is equal to the DOC content. Given that the DOM content of a water sample is approximately twice as high as its DOC concentration, this implies that only 50% of the DOM

present in these samples can complex with the REE. In view of the ultrafiltration data reported by Viers et al. (1997), this hypothesis might not be valid for the Mengong and Mar2 samples. Indeed, as shown in Table 3 of Viers et al. (1997), the REE concentrations extrapolated to a zero DOC concentration are positive, rather than negative as in the case of the newly ultrafiltered samples presented in our study. As shown above, calculated active DOM proportions range from 32 to 60% for the newly ultrafiltred samples, with a mean value of 50% fully in agreement with Tang and Johannesson's assumption (2003). Evidently, the situation is quite different for the Mengong and Mar2 samples, where ultrafiltration data suggest that 100% of the DOM present in these samples could be active in complexing the REE.

To test the role of this parameter on model results, we performed sensitivity analysis on the Mengong and Mar2 samples. Model predictions using an "active DOM parameter" set equal to 50%, as suggested by Tang and Johannesson (2003), were compared with results predicted using an "active DOM parameter" of 100%, as indicated by ultrafiltration studies of these samples. We performed the same sensitivity analysis on World Average River Water. However, the newly ultrafiltered samples were not treated, given that ultrafiltration studies of these samples clearly imply that their "active DOM parameter" must be equal to about 50%. Table 8 shows the results for Mengong and Mar2 samples. Overall, Table 8 shows that raising the "active DOM parameter" from 50 to 100% strongly increases the proportion of REE that are predicted to be complexed with HM in these two samples. The predicted increase occurs in both Model VI and SHM. Moreover, SHM predictions become similar to Model VI results for Mar2 sample (i.e., LnHM > 98%) and to ultrafiltration data. However, SHM predictions are still lower than ultrafiltration results for the more acidic Mengong sample. Fig. 7 presents the results of the sensitivity analysis on World Average River Water for La, Eu and Lu. We note a strong difference compared with the predictions obtained for this sample when using an "active DOM parameter" of 50%. More specifically, both SHM and Model VI indicate that ca. 100% of the REE should occur as humate complexes at a pH higher than 6.5. The only remaining noticeable difference is that SHM

continues to predict a slight deficit in LnHM species at low pH as compared to Model VI. This effect is known to be due to the lower extent of deprotonation of HM surfaces implied in SHM (see above).

Thus, raising the "active DOM parameter" from 50 to 100% leads to modifications in the modelling results that are far more important than those generated by differences in the electrostatic terms of the models or by uncertainties in the constant values for REE (see discussion in Tang and Johannesson, 2003) and/or competing cations. When the "active DOM parameter" is set to 100%, it is clearly not unexpected to observe a general increase in the proportion of the REE complexing with HM, as predicted both by Model VI and SHM. This increase in the "active DOM parameter" value is equivalent to enhancing the abundance of organic ligands in sample solutions, which can then quantitatively scavenge all the dissolved REE. The other important key point is that the change in "active DOM parameter" value leads to a strong reduction of the disparities produced in model predictions for World Average River Water, and the Mengong and Mar2 samples (compare Figs. 3 and 7, and Tables 5 and 8). Thus, by adopting an "active DOM parameter" of 100%, we obtain a fit between SHM and the ultrafiltration data for Mengong and Mar2 samples that is much better than previously established using a value of 50% for this parameter in SHM (see Tables 5 and 8).

Finally, two key questions arise from this study: what value should be adopted for the proportion of active DOM occurring in natural solutions (50 or 100%), and is this proportion constant from one natural solution to another? Considering the present ultrafiltration results and those obtained by Viers et al. (1997), it appears that the proportion of active DOM does not remain constant in waters, varying from 32 to 59% in the newly ultrafiltered samples, to 100% in the Mengong and Mar2 samples. A literature survey indicates that, in any case, this ratio could be significantly higher than the value of 50% used by Tang and Johannesson in their 2003 study. For example, a detailed study by Bryan et al. (2002) of the proportion of DOM that can complex metals (e.g., Cu and Al) in natural waters showed this amount to be ≈ 65% in most cases. This

proportion is clearly lower than the value of 100% set in our sensitivity analysis, but significantly higher than the value of 50% used by Tang and Johannesson (2003).

To conclude, the above sensitivity analysis indicates that it is critical to have prior knowledge of the amount of active DOM in a water before making use of SHM or Model VI to predict the speciation of REE in waters. This implies that ultrafiltration experiments and/or other analytical techniques able to determine the REE complexing capacity of DOM must be performed on the samples that we wish to model.

5. CONCLUSION

The scope of this study was to increase our understanding of how to describe REE-organic complexation in equilibrium speciation models. For this purpose, we compared the ability of SHM and Models V and VI to assess the role of DOM in the speciation of REE in organic-rich ground- and river waters. We used REE specific equilibrium constants estimated by LFER, applying complexation constants for REE with acetic acid. The advantage of testing SHM is that this model is part of a wider equilibrium model (Visual MINTEQ) that also allows modelling of dissolution/precipitation, sorption/desorption and oxidation/reduction. Both Model VI and SHM yield comparable results for World Average River Water, confirming the earlier finding that a large fraction of the dissolved REE in rivers occurs as organic complexes. This also suggests that the two models could be equally valuable for calculating REE speciation in low-DOC waters at circumneutral-pH. The two models also successfully reproduce ultrafiltration results obtained for acidic, DOC-rich ground- and river waters. However, the two models are found to yield slightly different results (depending on sample) when compared to newly obtained ultrafiltration results for organic-rich (DOC>7 mg L^{-1}) groundwaters at circumneutral pH, where Model VI predictions are in closer agreement with the ultrafiltration data than SHM. A survey of ultrafiltration results allows us to determine the "active DOM parameter" for the newly ultrafiltered water data. Thus,

the observed discrepancy between SHM predictions and ultrafiltration results cannot be due to the input of inappropriate "active DOM parameter" values in this model. Clearly, SHM appears to need some improvements to become a REE speciation model of universal application (i.e., also usable under acidic pH conditions). Moreover, sensitivity analysis indicates that the "active DOM parameter" is a key parameter for both Model VI and SHM. Consideration of previously published speciation results based on Model V shows that great care should be taken in making use of these results because of the possible introduction of inappropriate values for this parameter. The results presented in this study show that, before running speciation models, it is essential to know the proportion of DOM that is active in complexing REE in a given water sample. This requirement could severely complicate the use of models to assess the role of DOM in controlling the speciation of REE in natural waters.

Acknowledgements. We thank the technical staff at Rennes (M. Le Coz-Bouhnik, O. Hénin and P. Petitjean) for their assistance during the experimental and analytical work. Dr. M.S.N. Carpenter is acknowledged for English corrections. J.E. Sonke, K.H. Johannesson and several anonymous reviewers are thanked for thorough and constructive comments of an earlier version of this paper. This research was supported by the CPER programmes *"Développement de la Recherche sur la Maîtrise de la Qualité de l'Eau en Bretagne"* jointly funded by the French Government and the Council of Rennes Métropole.

APPENDIX 1 – Ultrafiltration procedure and chemical analyses

Samples were collected in November 2004 from shallow piezometers (0.5 to 1.5 m deep). The pH was measured in the field with a combined Sentix 50 electrode. The accuracy of pH measurements is estimated at ± 0.05 pH unit. About 60 mL of each sample were immediately filtered on site, through 0.2 µm cellulose acetate filter (Sartorius Minisart). An aliquot of 30 mL was acidified on site and subsequently used to measure major and trace cation concentrations. The remaining 30 mL were not acidified and used to measure alkalinity, major anions and DOC concentrations. For each sample, an extra 1 L aliquot was collected. This extra aliquot was filtered in the laboratory through 0.2 µm cellulose acetate membrane using a Sartorius Teflon filtration unit. Thirty mL of the filtrate were acidified and used to re-measure major and trace cation concentrations (including REE), while 10 mL were used to re-measure the major anions and DOC content. Ultrafiltration experiments were performed with the remaining filtrate. Ultrafiltrations were carried out with 15 mL centrifugal tubes equipped with permeable membranes of decreasing pore-size cut off (Millipore Amicon Ultra-15): 30 kDa, 10 kDa and 5 kDa. Each centrifugal filter device was washed and rinsed with HCl 0.1 N and MilliQ water two times before use. Centrifugations were performed using a Jouan G4.12 centrifuge equipped with swinging bucket, at 3000 g for between 20 (30 kDa and 10 kDa) and 30 (5 kDa) minutes, depending on the pore-size cut off. Each of the four investigated samples (PF1, PF3, F7 and F14) was ultrafiltered in duplicate. All experiments were performed at room temperature: 20±2 °C. Further information on the centrifugation procedure can be found in Pourret et al. (2007b).

Alkalinity was determined by potentiometric titration with an automatic titrator (794 Basic Titrino Methrom). Major anion (Cl^-, SO_4^{2-} and NO_3^-) concentrations were measured by ionic chromatography (Dionex DX-120). Major cation and trace element concentrations were determined by ICPMS (Agilent 4500), using indium as an internal standard. Dissolved organic carbon (DOC) was analysed on a total organic carbon analyzer (Shimadzu TOC-5050A). Typical

uncertainties on anion and cation measurements, as established from repeated analyses of standard solutions (SLRS 4 geostandard water solution for cations; K-biphtalate solutions for DOC; Dionex seven anions standard solutions for anions), are estimated at <±4% for anions and at <±5% for all other measured species.

All procedures (sampling, filtration, storing and analysis) were carried out in order to minimize contamination. Samples were stored in acid-washed Nalgene polypropylene containers before analyses. Blank concentrations for DOC and REE were <0.5 mg L^{-1} and <1 ng L^{-1}, respectively. All reported DOC concentrations are blank corrected (maximum correction = 8%). For the REE, there was no need for blank corrections, since the sample concentrations were systematically two to three orders of magnitude higher than blank levels. The instrumental error on REE analysis in our laboratory as established from repeated analyses of multi-REE standard solution (Accu Trace™ Reference, USA) and of the SLRS-4 water standard is <±2% (Dia et al., 2000; Davranche et al., 2004; Gruau et al., 2004; Davranche et al., 2005).

TABLE AND FIGURE CAPTIONS

Table 1. Log K for metal complexation with lactic acid (LA), acetic acid (AA) and first hydrolysis (OH), as well as log K_{MA} for HA and FA (from Tipping, 1998), used to obtain equations for LFER between log K_{MA} and log K for each ligand. Log K for AA, LA and OH are from NIST Database (Martell and Smith, 1998) for 25°C and zero ionic strength conditions.

Table 2. Log K_2 for metal complexation with lactic acid (LA), acetic acid (AA) and hydrolysis (OH), as well as log K_{Mb} for HA and FA (from Gustafsson and van Schaik, 2003), used to obtain equations for LFER between log K_{Mb} and log K_2 for each ligand. Log K values for LA, AA and OH are taken from NIST Database (Martell and Smith, 1998) at 25°C and zero ionic strength conditions.

Table 3. Summary of estimated log K_{MA} for the REE.

Table 4. Summary of estimated log K_{Mb} for the REE.

Table 5. Proportions of LnHM complexes calculated with Model V (Tang and Johannesson, 2003), Model VI and SHM for Mengong and Mar2 water samples. Fraction of LnHM complexes previously estimated for these two samples by ultrafiltration experiments are shown for comparison (Viers et al., 1997). The proportion of DOM active in complexing the REE is assumed to be 50% (i.e., active DOM content = DOC content).

Table 6. Comparison between the proportions of LnFA and LnHA complexes in PF1, PF3, F7 and F14 samples obtained by ultrafiltration experiments and modelling calculation using

Model VI and SHM. Proportions of DOM active in complexing the REE were calculated from ultrafiltration results (see text for further explanation).

Table 7. Model VI and SHM speciation calculations for Fe, Al and Ca in World Average River Water as a function of pH.

Table 8. Model VI and SHM predictions of the proportion of REE occurring as humate complexes in Mengong and Mar2 waters, with the "active DOM parameter" assumed to be equal to 100%. Ultrafiltration data shown for comparison are from Viers et al. (1997).

Table EA1. Values adopted in this study for Model VI parameters (based on Tipping, 1998).

Table EA2. Values adopted in this study for SHM parameters (based on Gustafsson, 2001b).

Table EA3. Concentrations of major solutes (in μmol L^{-1}), alkalinity (in μmol L^{-1}), REE (in nmol L^{-1}), and DOC (in mg L^{-1}) in ultrafiltered groundwaters.

Table EA4. Concentrations of trace metal (in μmol L^{-1}), REE (in nmol L^{-1}) and DOC (in mg L^{-1}) in the ultrafiltrates.

Fig. 1. Linear free-energy relationships between log K_{MA} and log K(LA), log K(AA) and log K(OH) listed in Table 2. Log K(LA), log K(AA) and log K(OH) are from the NIST Database (Martell and Smith, 1998), whereas log K_{MA} values are from Tipping (1998). Standard deviations are indicated where available. Dashed lines indicate 95% confidence intervals of linear fits. Shaded areas mark fields of available K(LA), log K(AA) and log K(OH) data.

Fig. 2. Linear free-energy relationships between log K_{Mb} and log K_2(LA), log K_2(AA) and log K_2(OH) listed in Table 5. The AA, LA and OH constants values are from the NIST Database (Martell and Smith, 1998), and the values of log K_{Mb} are from the "shmgeneric" Database (Gustafsson, 2001b). Dashed lines indicate 95% confidence intervals of linear fits. Shaded areas mark fields of available log K_2 (LA), log K_2 (AA) and log K_2 (OH) data.

Fig. 3. Model VI speciation calculations for (a) La, (b) Eu and (c) Lu in World Average River Water as a function of pH. The proportion of active DOM complexing the REE is assumed to be 50% (i.e., active DOM content = DOC content).

Fig. 4. SHM speciation calculations for (a) La, (b) Eu and (c) Lu in World Average River Water as a function of pH. The proportion of active DOM complexing the REE is assumed to be 50% (i.e., active DOM content = DOC content).

Fig. 5. ΣREE and Fe concentrations as a function of DOC concentrations in the successive filtrates (<0.2 µm, <30 kDa, <10 kDa, <5 kDa) for (a) PF3, (b) F7, (c) F14 and (d) PF1 water samples. Error bars correspond to standard deviations for two replicates, with some error bars being smaller than the symbol size. Point A represents the extrapolated amount of REE thought to be bound to humic matter, whereas point B gives the DOC content extrapolated to a REE content equal to 0 (see text for further explanation).

Fig. 6. Comparison of extent of proton dissociation for HA and FA calculated by Model VI and SHM as a function of pH.

Fig. 7. Model VI and SHM speciation calculations for (a) La, (b) Eu and (c) Lu for World Average River Water illustrating the effects of setting a value of 100% for the "active DOM parameter" on the proportion of REE complexed with HM in this sample, as a function of pH (see Figs. 3 and 4, for comparison).

REFERENCES

Aubert D., Stille P., and Probst A. (2001) REE fractionation during granite weathering and removal by waters and suspended loads: Sr and Nd isotopic evidence. *Geochim. Cosmochim. Acta* **65**, 387-406.

Bau M. (1999) Scavenging of dissolved yttrium and rare earths by precipitating iron oxyhydroxide: Experimental evidence for Ce oxidation, Y-Ho fractionation, and lanthanide tetrad effect. *Geochim. Cosmochim. Acta* **63**, 67-77.

Bidoglio G., Grenthe I., Qi P., Robouch P., and Omenetto N. (1991) Complexation of Eu and Tb with fulvic acids as studied by time-resolved laser induced fluorescence. *Talanta* **38**, 999-1008.

Brownlow A. H. (1996) Geochemistry. Prentice Hall, Englewood Cliffs, NJ.

Bryan S. E., Tipping E., and Hamilton-Taylor J. (2002) Comparison of measured and modelled copper binding by natural organic matter in freshwaters. *Comp. Biochem. Physiol. C* **133**, 37-49.

Byrne R. H. and Sholkovitz E. R. (1996) Marine chemistry and geochemistry of the lanthanides. In *Handbook on the Physics and Chemistry of Rare Earths* (eds. K.A. Gschneidner, Jr. and L.R. Eyring), Vol. 23, pp. 497-593. Elsevier Sciences B.V.

Coppin, F., Berger, G., Bauer, A., Castet, S. and Loubet, M., 2002. Sorption of lanthanides on smectite and kaolinite. Chemical Geology, 182: 57-68.

Davranche M., Pourret O., Gruau G., and Dia A. (2004) Impact of humate complexation on the adsorption of REE onto Fe oxyhydroxide. *J. Colloid Interface Sci.* **277**, 271-279.

Davranche M., Pourret O., Gruau G., Dia A., and Le Coz-Bouhnik M. (2005) Adsorption of REE(III)-humate complexes onto MnO_2: Experimental evidence for cerium anomaly and lanthanide tetrad effect suppression. *Geochim. Cosmochim. Acta,* **69**, 4825-4835.

De Baar H. J. W., German C. R., Elderfield H., and van Gaans P. (1988) Rare earth element distributions in anoxic waters of the Cariaco Trench. *Geochim. Cosmochim. Acta* **52**, 1203-1219.

De Baar H. J. W., Schijf J., and Byrne R. H. (1991) Solution chemistry of the rare earth elements in seawater. *Eur. J. Solid State Inorganic Chem.* **28**, 357-373.

Deberdt S., Castet S., Dandurand J.-L., Harrichoury J.-C., and Louiset I. (1998) Experimental study of $La(OH)_3$ and $Gd(OH)_3$ solubilities (25 to 150°C), and La-acetate complexing (25 to 80°C). *Chem. Geol.* **151**, 349-372.

Dia A., Gruau G., Olivié-Lauquet G., Riou C., Molénat J., and Curmi P. (2000) The distribution of rare earth elements in groundwaters: assessing the role of source-rock composition, redox changes and colloidal particle. *Geochim. Cosmochim. Acta* **64**, 4131-4151.

Dupré B., Viers J., Dandurand J.-L., Polvé M., Bénézeth P., Vervier P., and Braun J.-J. (1999) Major and trace elements associated with colloids in organic-rich river waters: ultrafiltration of natural and spiked solutions. *Chem. Geol.* **160**, 63-80.

Elderfield H. and Greaves M. J. (1982) The rare earth elements in seawater. *Nature* **296**, 214-219.

Elderfield H., Upstill-Goddard R., and Sholkovitz E. R. (1990) The rare earth elements in rivers, estuaries, and coastal seas and their significance to the composition of ocean waters. *Geochim. Cosmochim. Acta* **54**, 971-991.

Gosselin D. C., Smith M. R., Lepel E. A., and Laul J. C. (1992) Rare earth elements in chloride-rich groundwater, Palo Duro Basin, Texas, USA. *Geochim. Cosmochim. Acta* **56**, 1495-1505.

Gruau G., Dia A., Olivié-Lauquet G., Davranche M., and Pinay G. (2004) Controls on the distribution of rare earth elements in shallow groundwaters. *Wat. Res.* **38**, 3576-3586.

Gustafsson J. P. (2001a) Modeling the acid-base properties and metal complexation of humic substances with the Stockholm Humic Model. *J. Colloid Interface Sci.* **244**, 102-112.

Gustafsson J. P. (2001b) http://www.lwr.kth.se/english/OurSoftware/vminteq/index.htm.

Gustafsson J. P., Pechova P., and Berggren D. (2003) Modeling metal binding to soils: the role of natural organic matter. *Environ. Sci. Technol.* **37**, 2767-2774.

Gustafsson J. P. and van Schaik J. W. J. (2003) Cation binding in a mor layer: batch experiments and modelling. *European Journal of Soil Science* **54**, 295-310.

Ingri J., Widerlund A., Land M., Gustafsson O., Andersson P., and Ohlander B. (2000) Temporal variations in the fractionation of the rare earth elements in a boreal river; the role of colloidal particles. *Chem. Geol.* **166**, 23-45.

Janssen R. P. T. and Verweij W. (2003) Geochemistry of some rare earth elements in groundwater, Vierlingsbeek, The Netherlands. *Wat. Res.* **37**, 1320-1350.

Johannesson K. H., Farnham I. M., Guo C., and Stetzenbach K. J. (1999) Rare earth element fractionation and concentration variations along a groundwater flow path within a shallow, basin-fill aquifer, southern Nevada, USA. *Geochim. Cosmochim. Acta* **63**, 2697-2708.

Johannesson K. H. and Hendry M. J. (2000) Rare earth element geochemistry of groundwaters from a thick till and clay-rich aquitard sequence, Saskatchewan, Canada. *Geochim. Cosmochim. Acta* **64**, 1493-1509.

Johannesson K. H., Stetzenbach K. J., and Hodge V. F. (1997) Rare earth elements as geochemical tracers of regional groundwater mixing. *Geochim. Cosmochim. Acta* **61**, 3605-3618.

Johannesson K. H., Zhou X., Guo C., Stetzenbach K. J., and Hodge V. F. (2000) Origin of rare earth element signatures in groundwaters of circumneutral pH from southern Nevada and eastern California, USA. *Chem. Geol.* **164**, 239-257.

Johannesson K. H., Tang J., Daniels J. M., Bounds W. J., and Burdige D. J. (2004) Rare earth element concentrations and speciation in organic-rich blackwaters of the Great Dismal Swamp, Virginia, USA. *Chem. Geol.* **209**, 271-294.

Klungness G. D. and Byrne R. H. (2000) Comparative hydrolysis behavior of the rare earths and yttrium: the influence of temperature and ionic strength. *Polyhedron* **19**, 99-107.

Lead J. R., Hamilton-Taylor J., Peters A., Reiner S., and Tipping E. (1998) Europium binding by fulvic acids. *Anal. Chim. Acta* **369**, 171-180.

Lippold H., Müller N., and Kupsch H. (2005) Effect of humic acid on the pH-dependent adsorption of terbium(III) onto geological materials. *Appl. Geochem.* **20**, 1209-1217.

Luo Y.-R. and Byrne R. H. (2004) Carbonate complexation of Yttrium and the rare earth elements in natural rivers. *Geochim. Cosmochim. Acta* **68**, 691-699.

Maes A., De Brabandere J., and Cremers A. (1988) A modified Schubert method for the measurement of the stability of europium humic acid complexes in alkaline conditions. *Radiochim. Acta* **44/45**, 51-57.

Martell A. E. and Smith R. M. (1998) *NIST Critical Selected Stability Constants of Metal Complexes Database*, available at: http://www.nist.gov/srd/nist46.htm.

Milne C. J., Kinniburgh D. G., and Tipping E. (2001) Generic NICA-Donnan Model parameters for proton binding by humic substances. *Environ. Sci. Technol.* **35**, 2049-2059.

Milne C. J., Kinniburgh D. G., Van Riemsdijk W. H., and Tipping E. (2003) Generic NICA-Donnan model parameters for Metal-Ion binding by humic substances. *Environ. Sci. Technol.* **37**, 958-971.

Moulin V., Tits J., Moulin C., Decambox P., Mauchien P., and de Ruty O. (1992) Complexation behaviour of humic substances towards actinides and lanthanides studied by Time-Resolved Laser-Induced Spectrofluometry. *Radiochim. Acta* **58/59**, 121-128.

Nelson B. J., Wood S. A., and Osiensky J. L. (2004) Rare earth element geochemistry of groundwater in the Palouse Basin, northern Idaho-eastern Washington. *Geochemistry: Exploration, Environment, Analysis* **4**, 227-241.

Olivié-Lauquet G., Gruau G., Dia A., Riou C., Jaffrezic A., and Henin O. (2001) Release of trace elements in wetlands: role of seasonal variability. *Wat. Res.* **35**, 943-952.

Pourret O., Davranche M., Gruau G., and Dia A. (2007a) Competition between humic acid and carbonates for rare earth elements complexation. *J. Colloid Interface Sci.* **305**, 25-31.

Pourret O., Dia A., Davranche M., Gruau G., Hénin O., and Angée M. (2007b) Organo-colloidal control on major- and trace-element partitioning in shallow groundwaters: confronting ultrafiltration and modelling. *Appl. Geochem.* **doi: 10.1016:j.apgeochem.2007.02.007**

Ramsey J. B. (1969) Tests for specification errors in classical linear least-squares regression analysis. *Journal of the Royal Statistical Society, Series B* **XXXI** (Part 2), 350.

Schijf J. and Byrne R. H. (2004) Determination of $_{SO_4}\beta_1$ for yttrium and the rare earth elements at I = 0.66 m and t = 25 °C-Implications for YREE solution speciation in sulfate-rich waters. *Geochim. Cosmochim. Acta* **68**, 2825-2837.

Sholkovitz E. R. (1995) The aquatic chemistry of rare earth elements in rivers and estuaries. *Aquat. Geochem.* **1**, 1-34.

Smedley P. L. (1991) The geochemistry of rare earth elements in groundwater from the Carnmenellis area, southwest England. *Geochim. Cosmochim. Acta* **55**, 2767-2779.

Sonke J. E. and Salters V. J. M. (2006) Lanthanide-humic substances complexation. I. Experimental evidence for a lanthanide contraction effect. *Geochim. Cosmochim. Acta* **70**, 1495-1506.

Tang J. and Johannesson K. H. (2003) Speciation of rare earth elements in natural terrestrial waters: Assessing the role of dissolved organic matter from the modeling approach. *Geochim. Cosmochim. Acta* **67**, 2321-2339.

Tanikazi Y., Shimokawa T., and Nakamura M. (1992) Physicochemical speciation of trace elements in river waters by size fractionation. *Environ. Sci. Technol.* **26**, 1433-1444.

Tipping E. (1994) WHAM - A chemical equilibrium model and computer code for waters, sediments, and soils incorporating a discrete site/electrostatic model of ion-binding by humic substances. *Comput. Geosci.* **20**, 973-1023.

Tipping E. (1998) Humic Ion-Binding Model VI: an improved description of the interactions of protons and metal ions with humic substances. *Aquat. Geochem.* **4**, 3-48.

Tipping E. and Hurley M. A. (1992) A unifying model of cation binding by humic substances. *Geochim. Cosmochim. Acta* **56**, 3627-3641.

Tipping E., Rey-Castro C., Bryan S. E., and Hamilton-Taylor J. (2002) Al(III) and Fe(III) binding by humic substances in freshwaters, and implication for trace metal speciation. *Geochim. Cosmochim. Acta* **66**, 3211-3224.

Viers J., Dupré B., Polvé M., Schott J., Dandurand J.-L., and Braun J. J. (1997) Chemical weathering in the drainage basin of a tropical watershed (Nsimi-Zoetele site, Cameroon): comparison between organic-poor and organic-rich waters. *Chem. Geol.* **140**, 181-206.

Wood S. A. (1993) The aqueous geochemistry of the rare-earth elements: Critical stability constants for complexes with simple carboxylic acids at 25°C and 1 bar and their application to nuclear waste management. *Eng. Geol.* **34**, 229-259.

Yamamoto Y., Takahashi Y., and Shimizu H. (2005) Systematics of stability constants of fulvate complexes with rare earth ions. *Chemistry Letters* **34**, 880-881.

Yamamoto Y., Takahashi Y., and Shimizu H. (2006) Interpretation of REE patterns in natural water based on the stability constants. *Geochim. Cosmochim. Acta* **Goldschmidt Conference Abstracts**, doi:10.1016/j.gca.2006.06.1587.

Metals	log K (LA)	log K (AA)	log K(MOH)	log K_{MA} (HA)	log K_{MA} (FA)	ΔLK_2
Mg^{2+}	1.37	1.27	2.60	0.70	1.10	0.12
Ca^{2+}	1.45	1.18	1.30	0.70	1.30	0.0
Sr^{2+}	0.97	1.14	0.82	1.11	1.20	0.0
Mn^{2+}	1.43	1.4	3.40	0.60	1.70	0.58
Co^{2+}	1.90	1.46	4.35	1.10	1.40	1.22
Ni^{2+}	2.22	1.43	4.14	1.10	1.40	1.57
Cu^{2+}	3.02	2.22	6.50	2.00	2.10	2.34
Zn^{2+}	2.22	1.57	5.00	1.50	1.60	1.28
Cd^{2+}	1.70	1.93	3.09	1.30	1.60	1.48
Pb^{2+}	2.78	2.68	6.40	2.00	2.20	0.93
Al^{3+}	3.30	2.57	9.00	2.60	2.50	0.46

Table 1

Metals	log K_2(LA)	log K_2(AA)	log K_2(OH)	log K_{Mb}
Ca^{2+}	2.45	-	-	-11.30
Mn^{2+}	2.10	-	5.8	-
Cu^{2+}	4.84	3.63	11.8	-5.80
Zn^{2+}	3.75	1.36	10.2	-9.00
Cd^{2+}	2.74	2.86	7.7	-9.30
Pb^{2+}	3.61	4.08	10.9	-6.15
Al^{3+}	5.97	4.55	17.9	-4.20
Co^{2+}	3.07	1.10	9.2	-10.10

Table 2.

	log K_{MA} (HA)				log K_{MA} (FA)			
REE	From LA (Eqn. 1)	From AA (Eqn. 3)	From OH (Eqn. 5)	Adopted estimated values	From LA (Eqn. 2)	From AA (Eqn. 4)	From OH (Eqn. 6)	Adopted estimated values
La	2.30	2.20	1.54	2.20	2.30	2.27	1.80	2.27
Ce	2.45	2.25	1.66	2.25	2.40	2.31	1.88	2.31
Pr	2.46	2.30	1.66	2.30	2.40	2.35	1.88	2.35
Nd	2.47	2.32	1.69	2.32	2.41	2.37	1.90	2.37
Sm	2.53	2.50	1.77	2.50	2.45	2.49	1.96	2.49
Eu	2.56	2.42	1.79	2.42	2.47	2.44	1.97	2.44
Gd	2.54	2.31	1.78	2.31	2.46	2.36	1.96	2.36
Tb	2.56	2.20	1.82	2.20	2.47	2.27	1.99	2.27
Dy	2.55	2.13	1.83	2.13	2.47	2.23	2.00	2.23
Ho	2.59	2.09	1.84	2.09	2.49	2.20	2.01	2.20
Er	2.60	2.07	1.85	2.07	2.50	2.18	2.01	2.18
Tm	2.62	2.11	1.88	2.11	2.51	2.21	2.04	2.21
Yb	2.64	2.21	1.91	2.21	2.53	2.28	2.06	2.28
Lu	2.72	2.13	1.91	2.13	2.58	2.23	2.06	2.23

Table 3.

	log K_{Mb}			
REE	From LA (Eqn. 7)	From AA (Eqn. 8)	From OH (Eqn. 9)	Adopted estimated values
La	-5.74	-5.66	-7.82	-5.66
Ce	-5.02	-5.60	-7.65	-5.60
Pr	-4.68	-5.13	-7.59	-5.13
Nd	-4.55	-5.04	-7.53	-5.04
Sm	-4.32	-4.65	-7.36	-4.65
Eu	-4.15	-4.79	-7.36	-4.79
Gd	-4.41	-5.04	-7.25	-5.04
Tb	-4.11	-5.40	-7.19	-5.40
Dy	-3.83	-5.50	-7.13	-5.50
Ho	-3.70	-5.57	-7.08	-5.57
Er	-3.32	-5.65	-6.96	-5.65
Tm	-3.15	-5.71	-6.96	-5.71
Yb	-2.94	-5.30	-6.91	-5.30
Lu	-2.83	-5.50	-6.85	-5.50

Table 4.

	Mengong				Mar2			
	Ultrafiltration	Model V	Model VI	SHM	Ultrafiltration	Model V	Model VI	SHM
	% LnHM	% LnHM	% LnHM	% LnHM	% LnHM	% LnHM	% LnHM	% LnHM
La	86	63	60	39	94	87	99	95
Ce	86	72	65	40	94	91	99	95
Pr	87	76	71	55	96	92	100	97
Nd	86	77	74	59	95	93	100	98
Sm	100	86	90	71	100	96	100	99
Gd	100	80	73	52	100	94	100	98
Tb	100	77	60	46	100	93	99	95
Dy	100	75	52	43	100	92	99	94
Ho	100	75	48	41	100	92	98	93
Er	69	75	46	39	100	93	98	91
Tm	100	77	50	38	100	93	98	90
Yb	100	78	61	41	100	93	99	96
Lu	100	81	52	34	100	95	99	94

Table 5.

	PF3									F7								
	Ultrafiltration			SHM			Model VI			Ultrafiltration			SHM			Model VI		
	% LnHA	% LnFA	% LnHM	% LnHA	% LnFA	% LnHM	% LnHA	% LnFA	% LnHM	% LnHA	% LnFA	% LnHM	% LnHA	% LnFA	% LnHM	% LnHA	% LnFA	% LnHM
La	65	35	100	77	22	98	74	26	100	76	24	100	39	15	54	69	30	100
Ce	69	31	100	76	22	99	74	26	100	79	21	100	40	16	56	71	29	100
Pr	64	36	100	77	22	99	73	27	100	78	22	100	56	22	78	72	28	100
Nd	63	37	100	77	23	100	74	26	100	76	24	100	58	22	81	73	26	100
Sm	65	35	100	77	23	100	66	34	100	78	22	100	65	25	90	70	30	100
Eu	67	33	100	77	23	100	71	29	100	87	13	100	63	24	87	73	27	100
Gd	67	33	100	77	22	99	73	27	100	76	24	100	57	22	79	73	27	100
Tb	69	31	100	76	22	98	72	27	99	76	24	100	45	17	62	69	31	99
Dy	68	32	100	75	22	97	75	23	98	77	23	100	41	16	57	71	28	99
Ho	66	34	100	75	22	97	74	23	98	76	24	100	38	15	53	70	28	98
Er	63	37	100	74	22	96	73	24	97	75	25	100	34	13	47	68	30	98
Tm	63	38	100	73	22	95	72	25	97	74	26	100	31	12	43	69	30	98
Yb	61	39	100	70	21	90	71	27	98	71	29	100	45	17	62	69	30	99
Lu	58	42	100	74	22	96	72	26	97	68	32	100	38	15	53	70	29	99
	F14									PF1								
	Ultrafiltration			SHM			Model VI			Ultrafiltration			SHM			Model VI		
	% LnHA	% LnFA	% LnHM	% LnHA	% LnFA	% LnHM	% LnHA	% LnFA	% LnHM	% LnHA	% LnFA	% LnHM	% LnHA	% LnFA	% LnHM	% LnHA	% LnFA	% LnHM
La	83	17	100	72	7	79	61	38	100	73	27	100	67	13	79	80	20	100
Ce	91	9	100	72	7	80	62	38	100	71	29	100	63	12	75	81	19	100
Pr	83	17	100	83	8	92	62	38	100	75	25	100	73	14	87	81	19	100
Nd	83	17	100	84	8	93	64	36	100	76	24	100	74	14	89	82	18	100
Sm	83	17	100	88	9	97	57	43	100	75	25	100	78	20	98	78	22	100
Eu	84	16	100	87	9	95	61	39	100	89	11	100	78	15	94	81	19	100
Gd	82	18	100	84	8	92	63	37	100	81	19	100	73	14	87	81	18	100
Tb	83	17	100	76	8	83	61	38	99	83	17	100	60	12	72	78	22	100
Dy	83	17	100	72	7	79	64	35	99	75	25	100	53	10	64	80	20	99
Ho	82	18	100	70	7	77	63	35	98	77	23	100	50	10	60	78	21	99
Er	82	18	100	66	7	73	62	36	98	78	22	100	45	9	53	75	23	99
Tm	81	19	100	62	6	68	62	37	98	82	18	100	39	8	47	75	24	99
Yb	80	20	100	75	8	83	61	38	99	76	24	100	53	11	64	77	23	100
Lu	79	21	100	76	7	77	63	36	99	64	36	100	46	9	55	74	25	99

Table 6.

	% Fe-HM		% Al-HM		% Ca-HM	
pH	Model VI	SHM	Model VI	SHM	Model VI	SHM
3	10	31	19	1	0	0
3.5	15	41	38	2	0	0
4	16	45	56	7	1	0
4.5	15	42	71	26	1	0
5	13	34	81	64	1	0
5.5	12	25	82	85	1	1
6	10	16	75	90	2	1
6.5	10	9	53	85	2	1
7	10	5	17	62	2	1
7.5	9	3	2	27	2	1
8	7	2	0	8	2	2
8.5	4	1	0	2	3	2
9	2	0	0	0	3	2
9.5	1	0	0	0	3	2

Table 7.

	Mengong			Mar2		
	Ultrafiltration	Model VI	SHM	Ultrafiltration	Model VI	SHM
	% LnHM	% LnHM	% LnHM	% LnHM	% LnHM	% LnHM
La	86	98	85	94	100	99
Ce	86	98	86	94	100	99
Pr	87	99	92	96	100	99
Nd	86	99	94	95	100	99
Sm	100	100	93	100	100	100
Gd	100	99	94	100	100	99
Tb	100	98	75	100	100	98
Dy	100	97	71	100	100	98
Ho	100	96	69	100	100	98
Er	69	95	66	100	100	98
Tm	100	96	64	100	100	98
Yb	100	98	78	100	100	99
Lu	100	97	71	100	100	98

Table 8.

Parameter	Description	Values
n_A	Amount of type-A sites (mol g^{-1})	4.8 10^{-3} (FA), 3.3 10^{-3} (HA)
n_B	Amount of type-B sites (mol g^{-1})	0.5 x n_A
pK_A	Intrinsic proton dissociation constant for type-A sites	3.2 (FA), 4.1 (HA)
pK_B	Intrinsic proton dissociation constant for type-B sites	9.4 (FA), 8.8 (HA)
ΔpK_A	Distribution term that modifies pK_A	3.3 (FA), 2.1 (HA)
ΔpK_B	Distribution term that modifies pK_B	4.9 (FA), 3.6 (HA)
log K_{MA}	Intrinsic equilibrium constant for metal binding at type-A sites	Fitted from experimental data
log K_{MB}	Intrinsic equilibrium constant for metal binding at type-B sites	3.39 log K_{MA} -1.15
ΔLK_1	Distribution term that modifies log K_{MA}	2.8 (REE)
ΔLK_2	Distribution term that modifies the strength of bidentate and tridentate sites	0.55 log K_{NH3} = 0.29 (REE)
P	Electrostatic parameter	-115 (FA), -330 (HA)
K_{sel}	Selectivity coefficient for counterion accumulation	1
f_{prB}	Fraction of proton sites that can form bidentate sites	Calculated from geometry
f_{prT}	Fraction of proton sites that can form tridentate sites	Calculated from geometry
M	Molecular weight	1500 (FA), 15000 (HA)
r	Molecular radius	0.8 nm (FA), 1.72 nm (HA)

Table EA1.

Parameter	Description	Values
n_A	Amount of type-A sites (mol g^{-1})	5.4 10^{-3} (FA), 3.55 10^{-3} (HA)
n_B	Amount of type-B sites (mol g^{-1})	1.62 10^{-3} (FA), 1.78 10^{-3} (HA)
log K_A	Intrinsic proton dissociation constant for type-A sites	-3.51 (FA), -4.13 (HA)
log K_B	Intrinsic proton dissociation constant for type-B sites	-8.81 (FA), -8.99 (HA)
ΔpK_A	Distribution term that modifies log K_A	3.48 (FA), 3.03 (HA)
ΔpK_B	Distribution term that modifies log K_B	2.49 (FA), 3.03 (HA)
log K_{Mm}	Intrinsic equilibrium constant for monodentate complexation of metal M	Fitted from experimental data
log K_{Mb}	Intrinsic equilibrium constant for bidentate complexation of metal M	Fitted from experimental data
ΔLK_2	Distribution term that modifies the strength of complexation sites	1.3 (REE)
r	Molecular radius	0.75 nm (FA), 1.8 nm (HA)
C	Stern layer capacitance	2 F m^{-2}
N_s	Site density of HS functional groups	1.2 sites nm^{-2}
A_s	Specific surface area of HS	Calculated from geometry using r and N_s
g_f	Gel fraction parameters	0.72 (FA) 0.78 (HA)
K_C	Intrinsic equilibrium constant for accumulation of screening counterions	universal value: $10^{0.8}$

Table EA2.

	PF1	PF3	F7	F14
T (°C)	10.6	10.7	10.6	10.4
pH	7.08	6.93	6.19	6.4
Cl	1340.00	1040.00	1949.99	1490.00
SO4	106.56	89.23	642.56	364.65
NO3	33.72	740.89	9.19	6.93
DOC	17.25	7.66	11.12	21.49
Na	628.10	555.03	1526.33	868.21
Mg	737.71	513.06	459.99	266.45
Al	3.97	2.71	0.59	3.97
K	12.58	8.21	14.02	7.70
Ca	213.75	161.03	722.55	609.78
Fe	17.10	1.77	25.62	44.08
Mn	0.56	0.18	21.72	9.32
La	1.27	5.79	3.73	10.00
Ce	2.60	13.48	9.27	22.16
Pr	0.39	1.81	1.24	3.02
Nd	1.66	7.66	5.63	12.67
Sm	0.33	1.29	1.34	2.93
Eu	0.07	0.24	0.27	0.61
Gd	0.26	0.86	1.31	2.73
Tb	0.03	0.08	0.18	0.38
Dy	0.16	0.41	1.12	2.23
Ho	0.03	0.08	0.24	0.43
Er	0.09	0.21	0.77	1.22
Tm	0.01	0.03	0.11	0.17
Yb	0.09	0.18	0.71	1.05
Lu	0.02	0.03	0.12	0.16
Alkalinity	1867	385	1318	623

Table EA3.

	PF3				F7				F14				PF1			
	0.2 µm	30 kDa	10 kDa	5 kDa	0.2 µm	30 kDa	10 kDa	5 kDa	0.2 µm	30 kDa	10 kDa	5 kDa	0.2 µm	30 kDa	10 kDa	5 kDa
La	5.79	4.14	3.12	2.01	3.73	1.31	1.09	0.60	10.00	2.97	1.77	0.79	1.27	0.21	0.15	0.08
Ce	13.48	9.63	7.22	4.20	9.27	3.08	2.52	1.30	22.16	6.27	3.55	0.95	2.60	0.42	0.32	0.17
Pr	1.81	1.31	0.99	0.66	1.24	0.44	0.36	0.19	3.02	0.93	0.54	0.24	0.39	0.08	0.05	0.03
Nd	7.66	5.73	4.33	2.85	5.63	2.19	1.81	1.00	12.67	4.16	2.50	1.13	1.66	0.36	0.29	0.12
Sm	1.29	0.94	0.68	0.46	1.34	0.56	0.45	0.24	2.93	1.01	0.61	0.27	0.33	0.09	0.07	0.03
Eu	0.24	0.17	0.13	0.08	0.27	0.11	0.09	0.03	0.61	0.21	0.12	0.05	0.07	0.02	0.02	0.00
Gd	0.86	0.61	0.46	0.29	1.31	0.60	0.48	0.27	2.73	1.04	0.62	0.28	0.26	0.08	0.06	0.02
Tb	0.08	0.06	0.04	0.03	0.18	0.08	0.06	0.03	0.38	0.15	0.09	0.04	0.03	0.01	0.01	0.00
Dy	0.41	0.30	0.22	0.13	1.12	0.52	0.40	0.23	2.23	0.87	0.54	0.24	0.16	0.05	0.04	0.02
Ho	0.08	0.06	0.04	0.03	0.24	0.12	0.10	0.06	0.43	0.19	0.12	0.05	0.03	0.01	0.01	0.00
Er	0.21	0.16	0.12	0.08	0.77	0.40	0.33	0.19	1.22	0.55	0.37	0.16	0.09	0.04	0.03	0.01
Tm	0.03	0.02	0.02	0.01	0.11	0.06	0.05	0.03	0.17	0.08	0.05	0.02	0.01	0.01	0.00	0.00
Yb	0.18	0.14	0.11	0.07	0.71	0.42	0.35	0.21	1.05	0.53	0.36	0.17	0.09	0.04	0.03	0.01
Lu	0.03	0.03	0.02	0.01	0.12	0.08	0.06	0.04	0.16	0.09	0.06	0.03	0.02	0.01	0.01	0.00
ΣREE	32.15	23.30	17.48	10.89	26.04	9.97	8.15	4.41	59.78	19.04	11.29	4.44	7.00	1.41	1.09	0.52
DOC	7.66	6.66	5.66	4.97	11.12	8.14	7.93	6.58	21.49	16.28	14.38	10.55	17.25	15.73	14.27	13.48
Al	2.69	0.67	0.57	0.39	0.58	0.28	0.22	0.13	3.97	1.58	1.16	0.60	0.93	0.43	0.38	0.24
Mn	0.18	0.16	0.16	0.05	21.72	22.88	22.56	20.99	9.32	7.77	7.72	0.24	0.56	0.46	0.46	0.18
Fe	1.77	0.21	0.48	0.00	25.62	0.97	0.48	0.11	44.08	5.19	1.36	0.41	17.10	0.63	0.41	0.11

Table EA4.

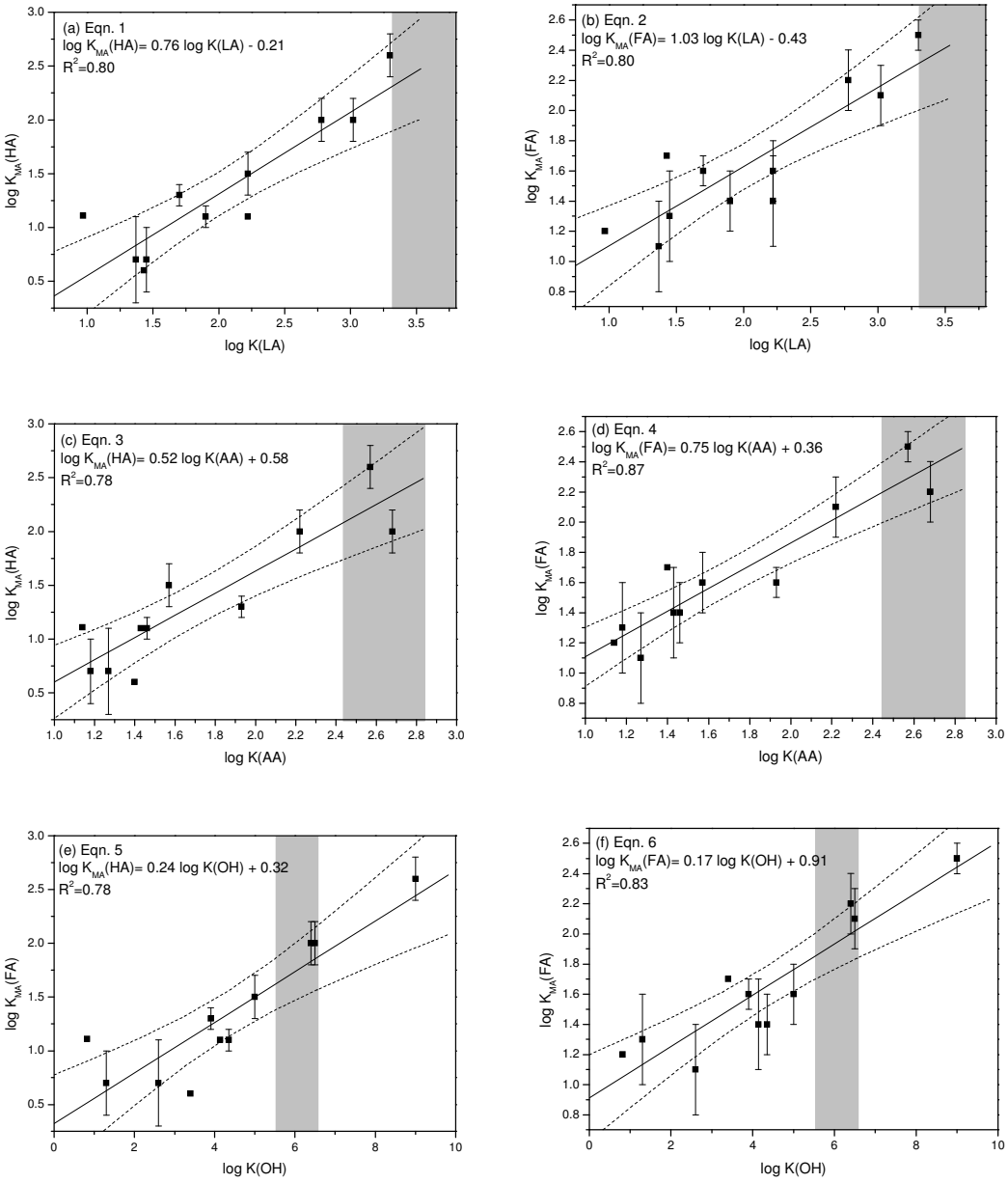
(a) Eqn. 1
log K_MA(HA)= 0.76 log K(LA) - 0.21
R²=0.80
log K_MA(HA)
log K(LA)
(b) Eqn. 2
log K_MA(FA)= 1.03 log K(LA) - 0.43
R²=0.80
log K_MA(FA)
log K(LA)
(c) Eqn. 3
log K_MA(HA)= 0.52 log K(AA) + 0.58
R²=0.78
log K_MA(HA)
log K(AA)
(d) Eqn. 4
log K_MA(FA)= 0.75 log K(AA) + 0.36
R²=0.87
log K_MA(FA)
log K(AA)
(e) Eqn. 5
log K_MA(HA)= 0.24 log K(OH) + 0.32
R²=0.78
log K_MA(FA)
log K(OH)
(f) Eqn. 6
log K_MA(FA)= 0.17 log K(OH) + 0.91
R²=0.83
log K_MA(FA)
log K(OH)

Fig. 1.

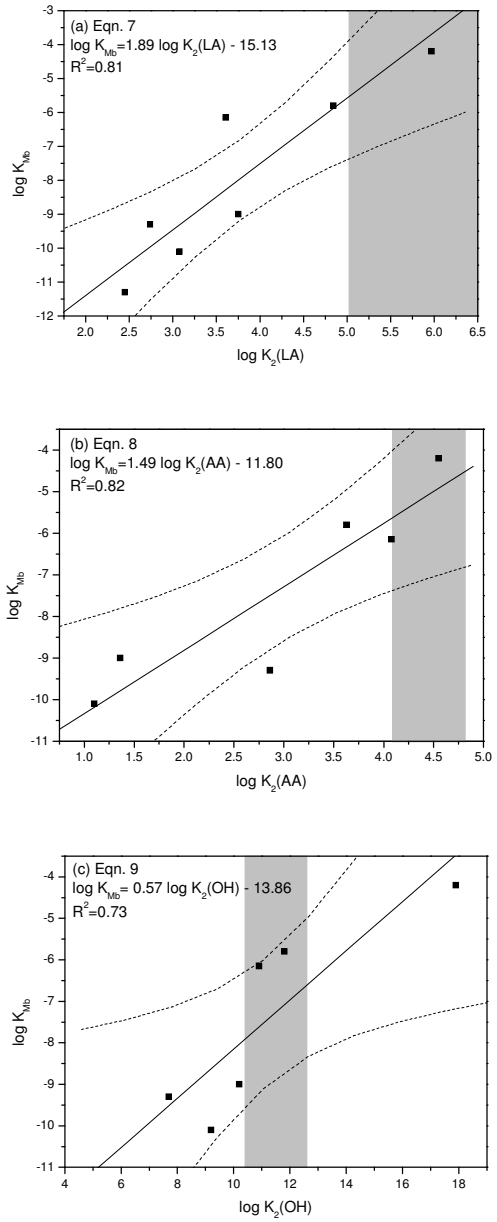
(a) Eqn. 7
log K_Mb=1.89 log K_2(LA) - 15.13
R^2=0.81
log K_Mb
log K_2(LA)
(b) Eqn. 8
log K_Mb=1.49 log K_2(AA) - 11.80
R^2=0.82
log K_Mb
log K_2(AA)
(c) Eqn. 9
log K_Mb= 0.57 log K_2(OH) - 13.86
R^2=0.73
log K_Mb
log K_2(OH)

Fig. 2.

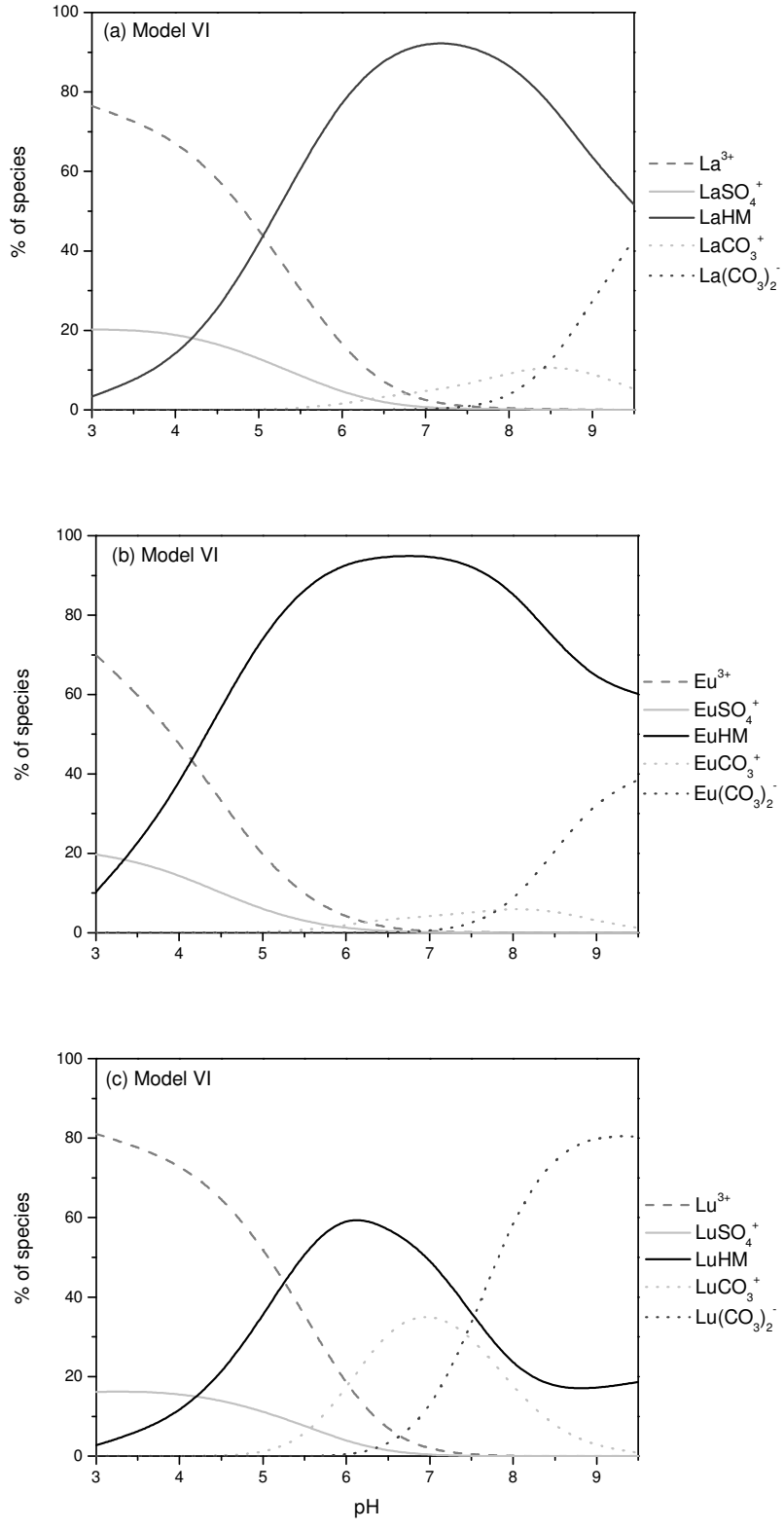
(a) Model VI
% of species
La3+
LaSO4+
LaHM
LaCO3+
La(CO3)2-
(b) Model VI
% of species
Eu3+
EuSO4+
EuHM
EuCO3+
Eu(CO3)2-
(c) Model VI
% of species
Lu3+
LuSO4+
LuHM
LuCO3+
Lu(CO3)2-
pH

Fig. 3.

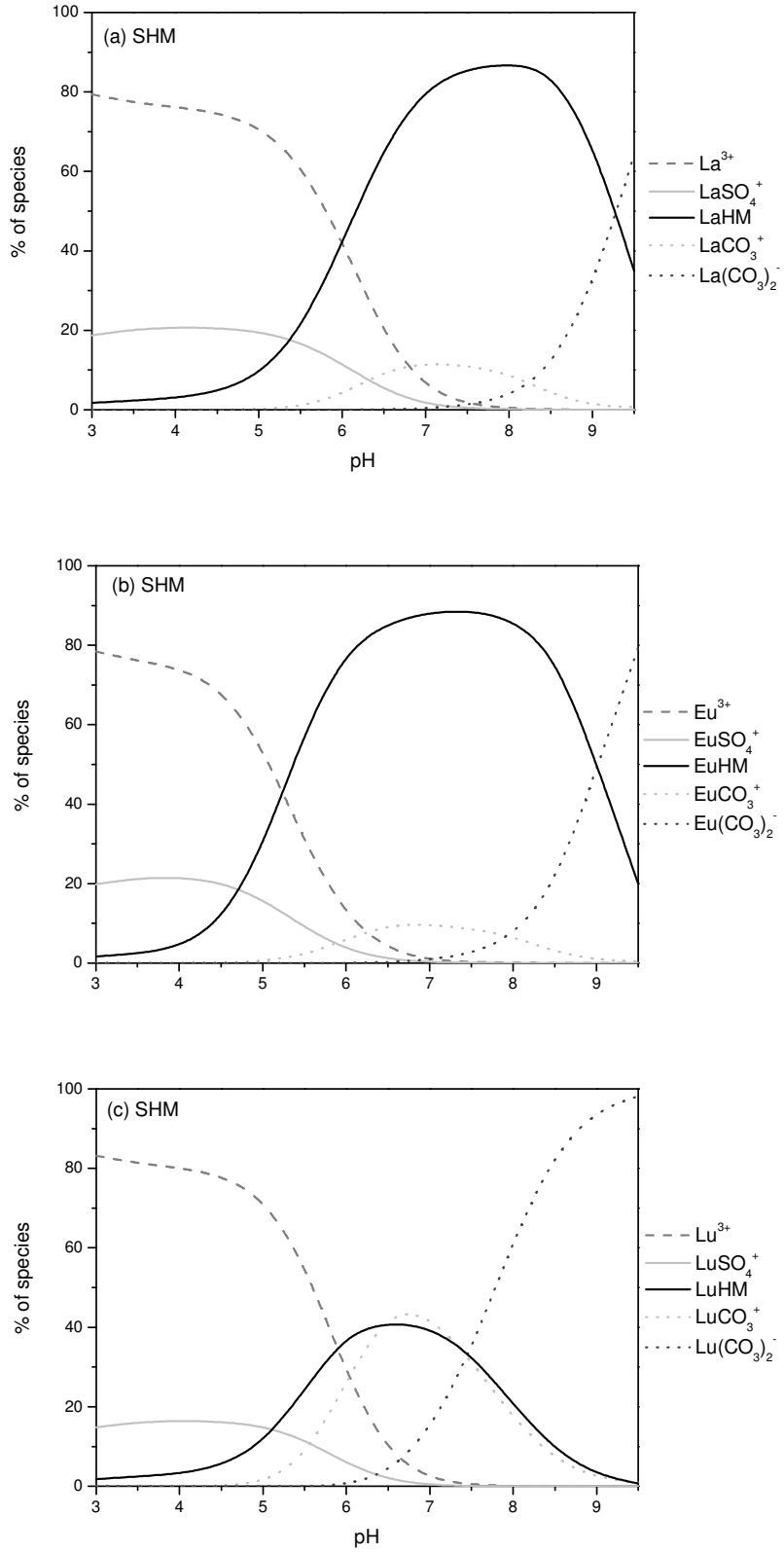
(a) SHM
% of species
pH
La3+
LaSO4+
LaHM
LaCO3+
La(CO3)2-
(b) SHM
% of species
pH
Eu3+
EuSO4+
EuHM
EuCO3+
Eu(CO3)2-
(c) SHM
% of species
pH
Lu3+
LuSO4+
LuHM
LuCO3+
Lu(CO3)2-

Fig. 4.

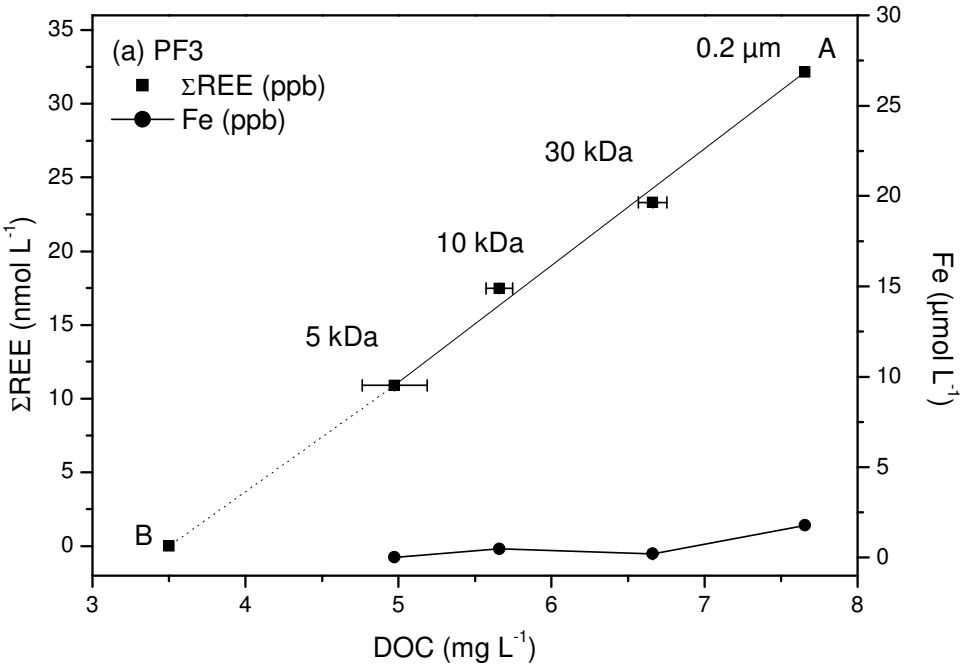
(a) PF3
ΣREE (ppb)
Fe (ppb)
0.2 µm
A
30 kDa
10 kDa
5 kDa
B
ΣREE (nmol L-1)
Fe (µmol L-1)
DOC (mg L-1)

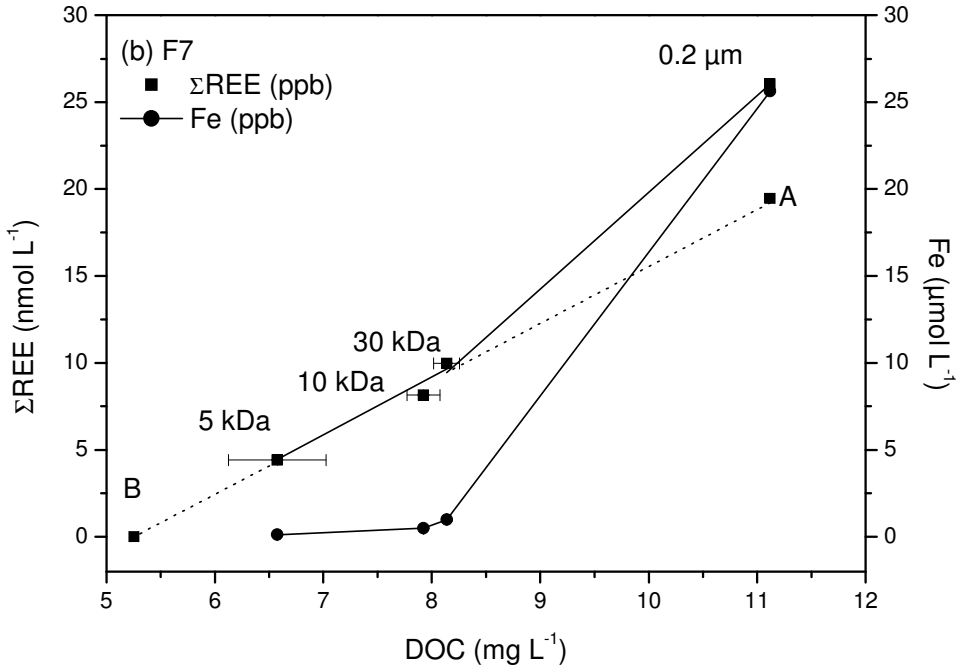
(b) F7
ΣREE (ppb)
Fe (ppb)
0.2 µm
A
30 kDa
10 kDa
5 kDa
B
ΣREE (nmol L-1)
Fe (µmol L-1)
DOC (mg L-1)

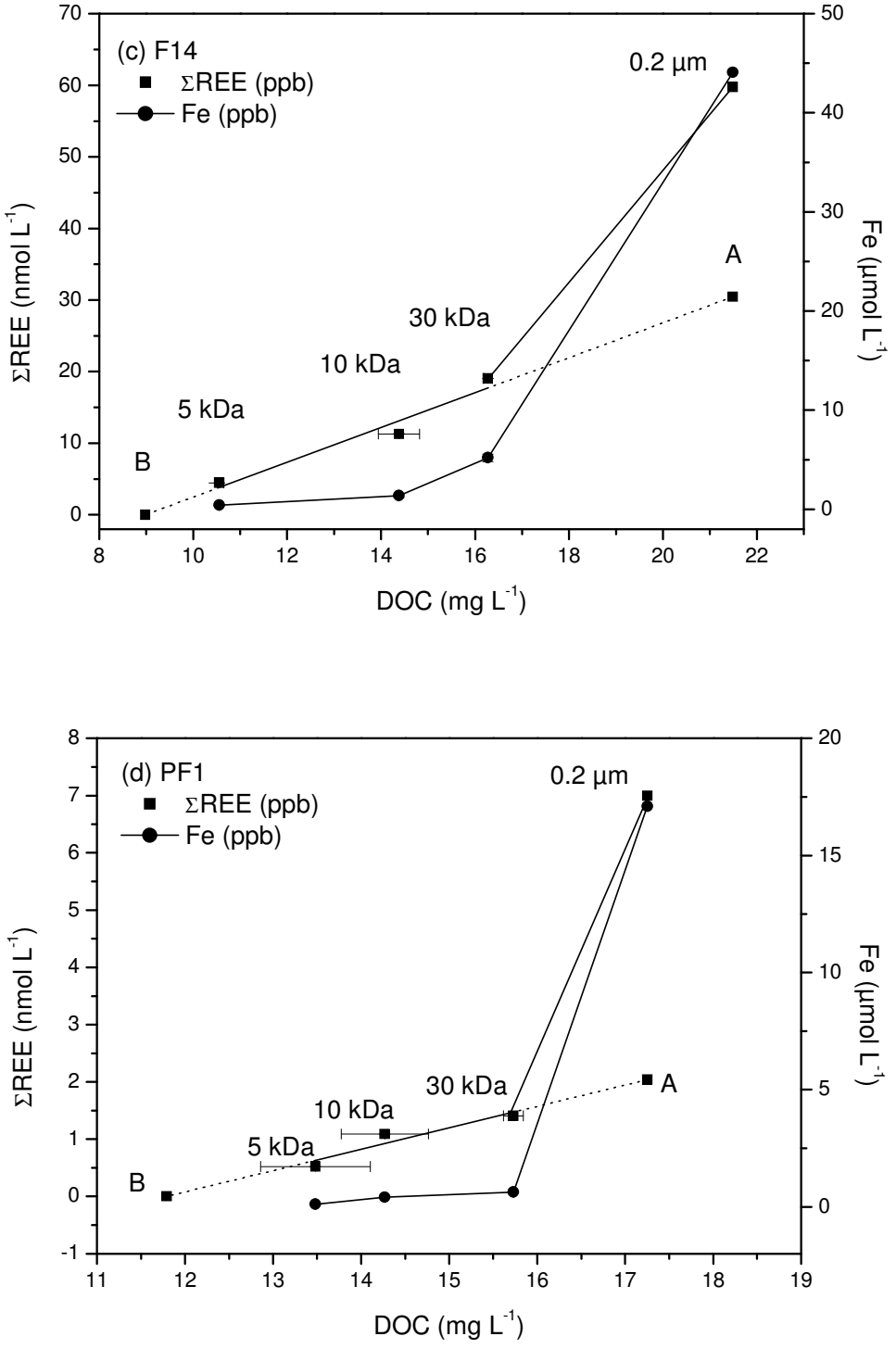
(c) F14
ΣREE (ppb)
Fe (ppb)
0.2 µm
A
30 kDa
10 kDa
5 kDa
B
ΣREE (nmol L-1)
Fe (µmol L-1)
DOC (mg L-1)
(d) PF1
ΣREE (ppb)
Fe (ppb)
0.2 µm
A
30 kDa
10 kDa
5 kDa
B
ΣREE (nmol L-1)
Fe (µmol L-1)
DOC (mg L-1)

Fig. 5.

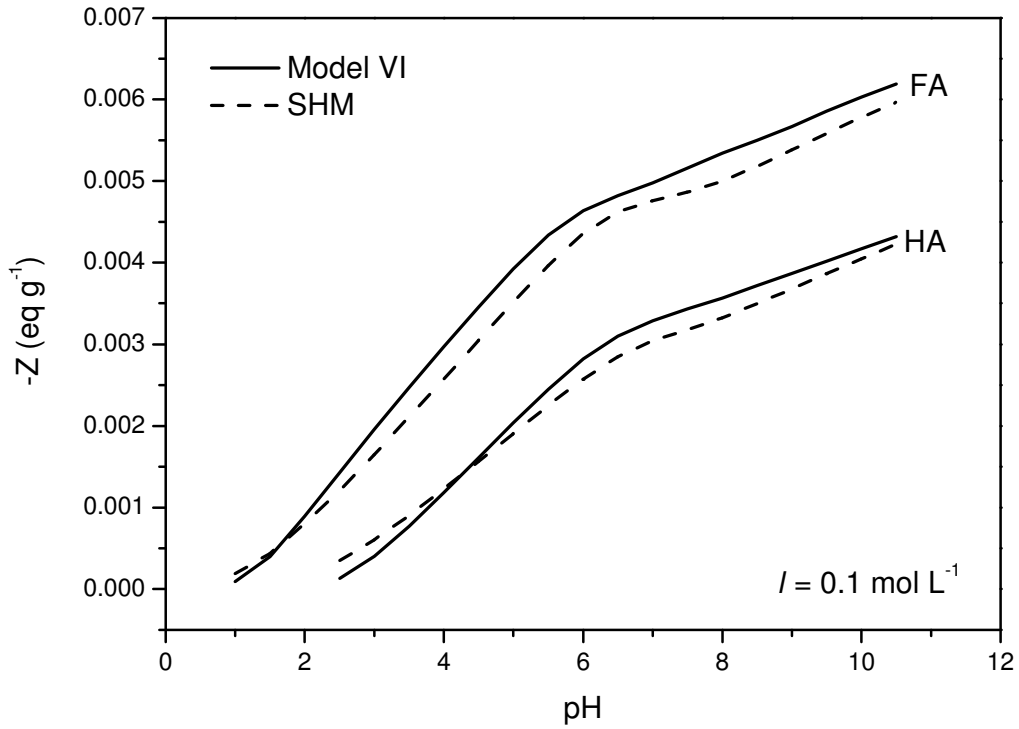
Model VI
SHM
FA
HA
I = 0.1 mol L-1
-Z (eq g-1)
pH
0.000
0.001
0.002
0.003
0.004
0.005
0.006
0.007
0
2
4
6
8
10
12

Fig. 6.

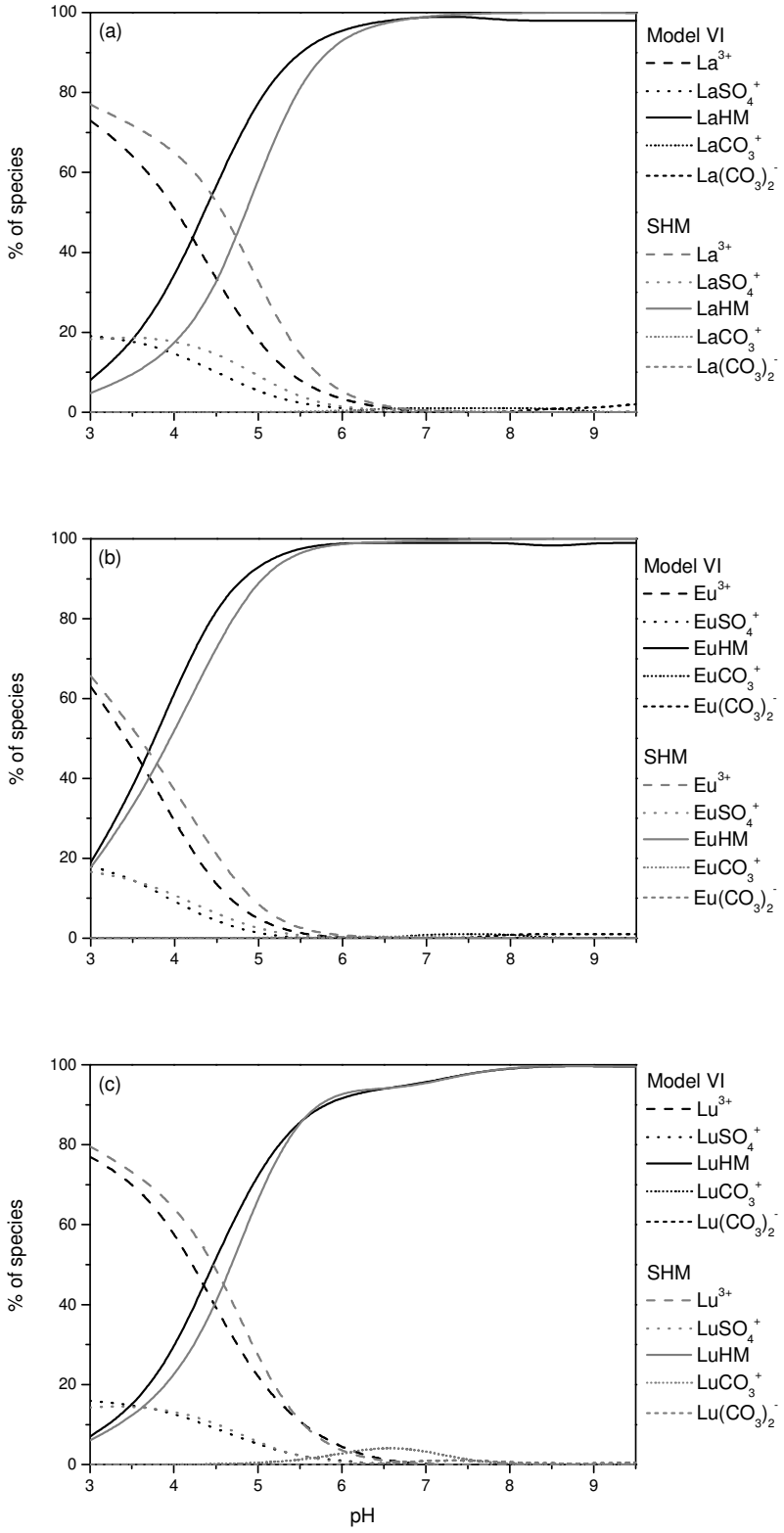
(a)
(b)
(c)
% of species
pH
Model VI
SHM
La3+
LaSO4+
LaHM
LaCO3+
La(CO3)2-
Eu3+
EuSO4+
EuHM
EuCO3+
Eu(CO3)2-
Lu3+
LuSO4+
LuHM
LuCO3+
Lu(CO3)2-

Fig. 7.